International Atomic Energy Agency

INDC(GDR)-22
Distribution: L

INDC INTERNATIONAL NUCLEAR DATA COMMITTEE

INDC(GDR)-22

Consistent Interpretation of Neutron-Induced Charged-Particle Emission in Silicon

D. Hermsdorf

Technical University of Dresden
Department of Physics

June 1982

IAEA NUCLEAR DATA SECTION, WAGRAMERSTRASSE 5, A-1400 VIENNA

Printed by the IAEA in Austria
July 1983
83-03743

INDC(GDR)-22
Distribution: L

Consistent Interpretation of Neutron-Induced Charged-Particle Emission in Silicon

D. Hermsdorf

Technical University of Dresden
Department of Physics

June 1982

Consistent Interpretation of Neutron-Induced Charged-Particle Emission in Silicon

D. Hermsdorf

Abstract

Users requesting gas production cross sections for Silicon will be confronted with serious discrepancies taking evaluated data as well as experimental ones. To clarify the accuracies achieved at present in experiments and evaluations in this paper an intercomparison of different evaluated nuclear data files has been carried out resulting in recommendations for improvements of these files. The analysis of the experimental data base also shows contradictory measurements or in most cases a lack of data. So an interpretation of reliable measured data in terms of nuclear reaction theories has been done using statistical and direct reaction mechanism models. This study results in a consistent and comprehensive evaluated data set for neutron-induced charged-particle production in Silicon which will be incorporated in file 2015 of the SOKRATOR library.

1. Introduction

Silicon is of real importance from aspects of radiation shielding as well as from measuring techniques and microelectronics. Whereas from radiation shielding point of view neutron, charged-particle and γ-production cross sections are of interest /1/, for studies of the solid state properties of Silicon the charged-particle production cross sections will be needed. However, Silicon is also of highly interest from fundamental nuclear physics.

Due to the relative low-mass nucleus Si the neutron-induced emission of charged particles will be comparable with the neutron emission itself and effects will be expected resulting from competitions between different reaction channels and mechanisms at least at energies above 10 MeV.

So, an analysis of the substantiated knowledge on charged-particle production in Silicon should yield a better meet the user's data requests as well as an improved elucidation of reaction mechanisms in medium mass nuclei. Although the nucleus Silicon is an excellent object for investigations because it may be part of the measuring technique itself, the degree of confidence of experimental data collected up to now is unsatisfactory. Usually the situation will be characterized by scarce and contradictory data.

This is the reason why only particular results have been studied in terms of nuclear theory. There is no attempt in literature to try a consistent interpretation of all existing experimental data.

Reflecting this status all evaluated nuclear data files available for users normally exhibit strong deviations from each other and are incomplete in that sense they are not giving angular distributions and energy spectra for charged particles. In contrast to this requests for angular and energy differential data have been compiled in WRENDA /1/ for radiation damage calculations in fusion reactor design studies and for solid state physics applications.

To overcome these difficulties and uncertainties this paper was devoted to yield more reliable and complete data for most important charged-particle cross-sections in Silicon.

2. Present status of evaluated nuclear data files

Silicon is included in different evaluated nuclear data libraries. For an intercomparison data have been taken from UKNDL, ENDL, ENDF/B and JENDL as well as from the dosimetry file SAND-II.

It could be shown formerly by the author /2/ that there is no real independent re-evaluation or new evaluation since 1975. In all cases of the release of any new version of a nuclear data file (or library) only small corrections and additions have been observed. This remark may not be true for the version ENDF/B-V.

But this couldn't prooved by the author because of the confinement of this library for many users.

Fig. 1

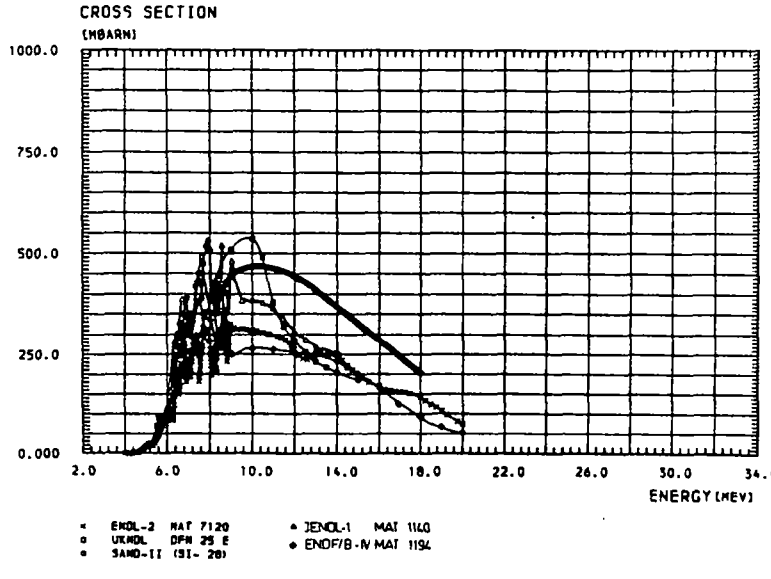

Generally, the data for charged-particle production evaluated for MAT 1194 of ENDF/B-IV are the most complete massive given in any library. Only there partial excitation functions, angular

distributions of protons, alpha-particles and deuterons as well as particle spectra can be found. No data for the emission of tritons and ^{3}He are known.

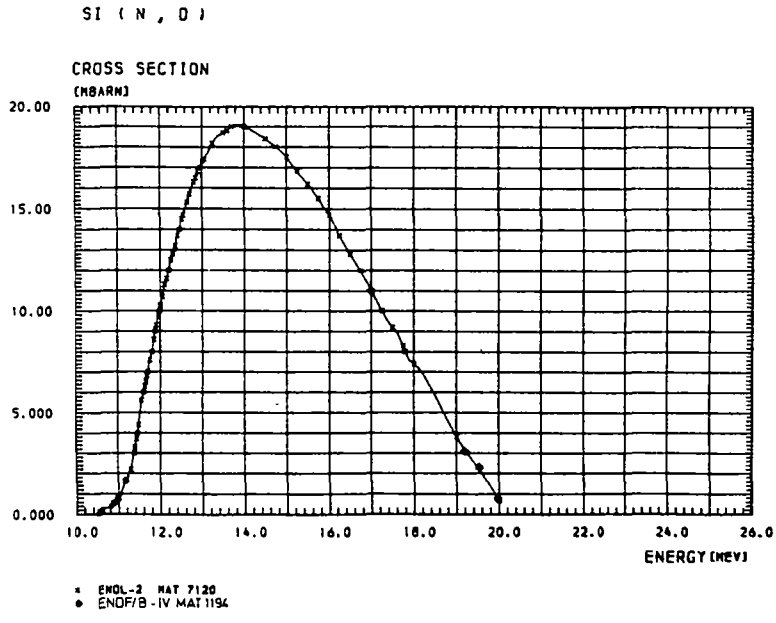

Fig.2

If we look for the agreement of data obtained from several libraries serious contradictions can be discovered for quantities like excitation functions for (n,p), (n,α) and (n,d). This is illustrated in figs. 1 to 3. No normal user can recognize the most relevant curve from this confusing situation without detailled knowledge of the accuracy achieved now. A warning should be given for use of any evaluation carried out before 1975.

We concluded /2/ from this analysis to create a new evaluation for Silicon. All data shown in the course of this paper will be incorporated in file 2015 of the library SOKRATOR maintained at CJD Obninsk in the format ENDF/B now.

Fig. 3

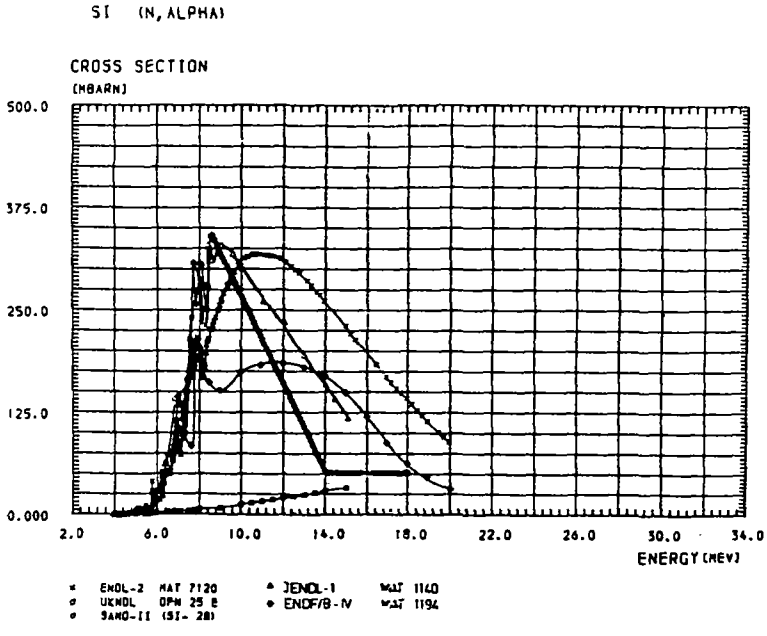

3. $^{28}Si(n,p)^{28}Al$

3.1. Review of experimental data base

The proton production in natural Silicon may exclusively determined by the $^{28}Si(n,p)^{28}Al$ (Q =-3.85 MeV) reaction because of considerable higher Q-values for ^{29}Si and ^{30}Si of the order of -2.9 MeV and -7.7 MeV respectively.

Further, the experimental techniques applied for the study of $^{28}Si(n,p)$ may be twofold. The reaction can be observed by the activation method as well as by the spectrum method providing for partial informations. Using both, a lot of data points for the total excitation function and partial excitation functions for several discrete proton transitions have been measured from threshold up to about 22 MeV.

Unfortunately the level schema of the residual odd-odd nucleus $^{28}_{13}Al_{15}$ doesn't favour this investigation because of some unresolvable states. Normally only proton groups of two ore more transitions can be obtained by the proton-spectrometry method.

The actual situation will be summarized in figs. 4 to 6 using experiments by several authors /3 to 14/.

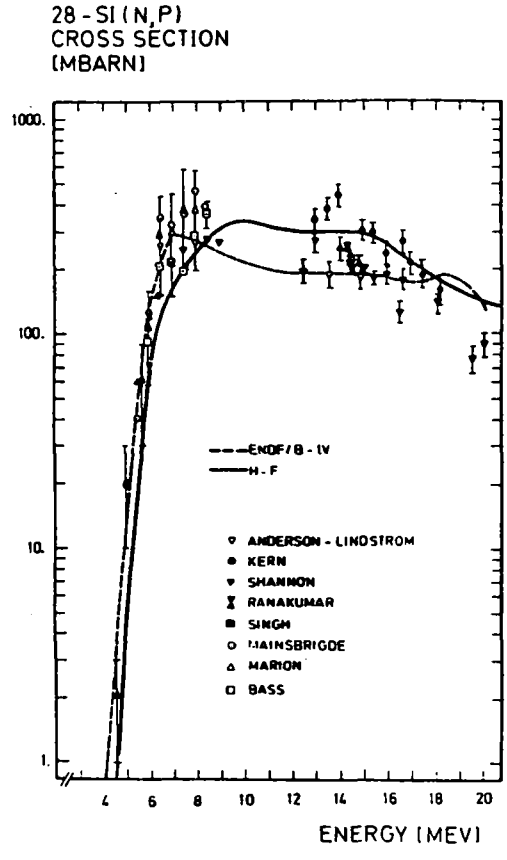

Fig. 4

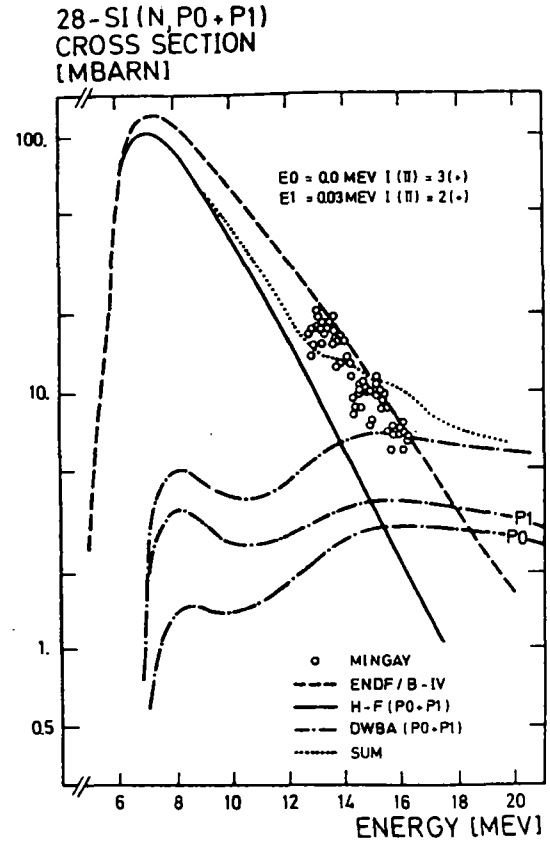

Fig. 5

In accordance to the resolution in respect to the neutron incident energy strongly fluctuating cross sections will be observed in both methods with widths of about 50-100 keV. This results from an intermediate structure of the compound nucleus ^{29}Si.

On the other hand our knowledge on angular distributions and proton energy spectra is considerably more incomplete. Besides some measurements around 14 MeV neutron incidence energy /15, 16, 17, 18/ single experiments at energies from 7 to 9 MeV /19/ have been reported for the first proton groups p_0+p_1 (figs.6,7).

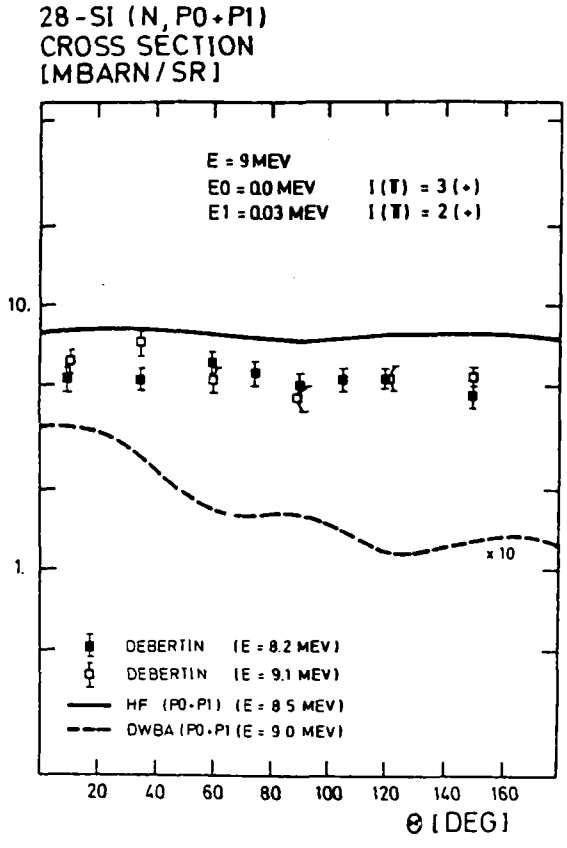

Fig. 6

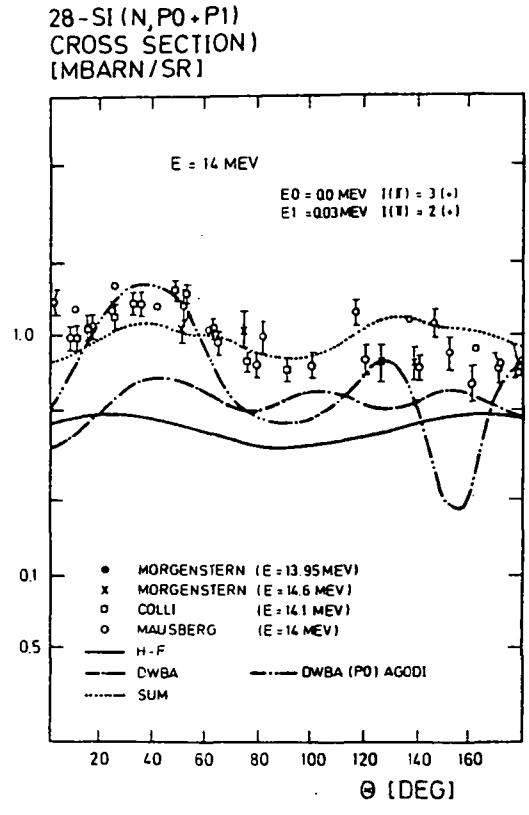

Fig. 7

Especially at 14 MeV the experimental data spread considerably reflecting the fluctuations in the excitation functions of the p_0 and p_1 transitions. Looking on that scarce informations (shown in figs. 6 and 7) a special feature will be seen clearly in all angular distribution of the p_0+p_1-group. This is a bump around 40-50 degrees which increases with ascending neutron energy indicating deviations from flat angular distributions predicted by the statistical model. This is a typically feature attributed to direct reactions with a definite transfer of angular momentum L.

Also the angular distributions of higher proton groups show remarkable asymmetric behaviours as was found experimentally by Morgenstern etal. /15/.

Unfortunately angular distributions at higher neutron energies and for other proton groups havn't been published up to now.

Further a decisive gap of proton emission spectra data exists. This may be caused by a very complex particle spectrum seen by the Si-detectors which will be used as target at the same time coming from competitive p, d and α particle emitting reactions within. Only one reliable experiment could be found at 21.6 MeV /20/ yielding double differential cross sections in an angular range from 0 to 60 degrees and proton emission energies between 4 and 11 MeV. Looking at the behaviour of p_0+p_1-group a clear dependence on angle can be observed substantiating the assumption of contributions from direct direction mechanisms in (n,p_i) particle cross sections. From an integration over solid angle 4π and energy a value in good agreement with data obtained by integral measurements (compare fig. 4) can be obtained. Therefore, the normalization used in this experiment relative to a value of σ_{n,α_0} at 21.6 MeV seems to be satisfied (see part 5.3 of this paper).

Fig. 8

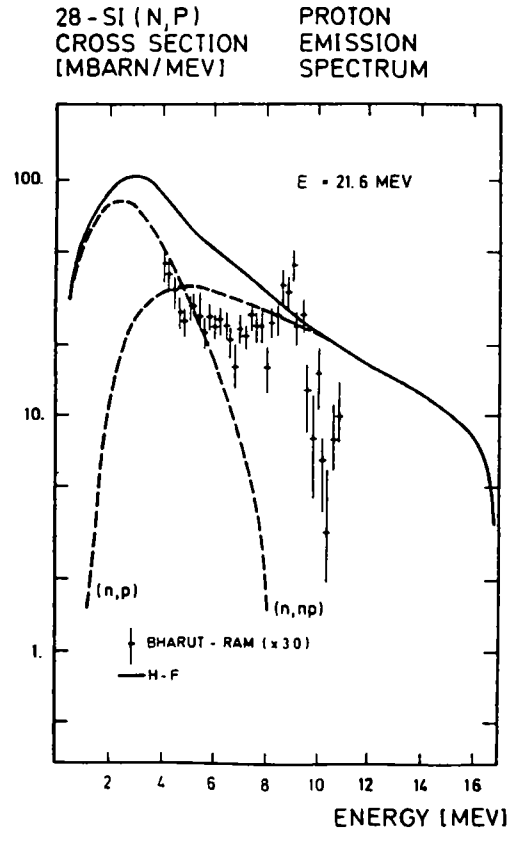

In all other cases absolute measurements have been choosen to allow an independend comparison with calculated cross sections.

3.2. Interpretation of experimental data in terms of reaction model calculations

3.2.1. Application of statistical model

After the introduction in the analysis of nuclear reactions proceeding via a compound nucleus formation and its decay the statistical model has been proved to be a very powerful method for description of a great body of experimental informations. Nevertheless, any application for a special nucleus preassumes the test of following two conditions

i) the ratio $\langle\Gamma\rangle / \langle D\rangle$ for the compound nucleus in the excitation energy range considered

and

ii) the determination of optical model parameters for all particles involved in all open channels for the decay of vompound nucleus states.

Whereas the second one can be fulfilled by a normal parameter adjustment procedure using optical model codes the first one results in a limitation of either the excitation energy range or the mass range of the nuclei to be studied.

^{28}Si is known to exhibit a strong resonance structure in the energy range from about 0.5 up to 15 MeV which corresponds to an excitation energy range in ^{29}Si in the order of 9 to 23 MeV. From neutron total and elastic scattering cross sections /21, 22/ averaged values of $\langle\Gamma\rangle \approx 500$ keV and $\langle D\rangle \approx 500$ keV can be deduced at about 1 MeV. So an application of the statistical model in the case of ^{28}Si may be doubtful but it has been done nevertheless with encouraging results. If it has been done also in this paper two facts should be kept in mind:

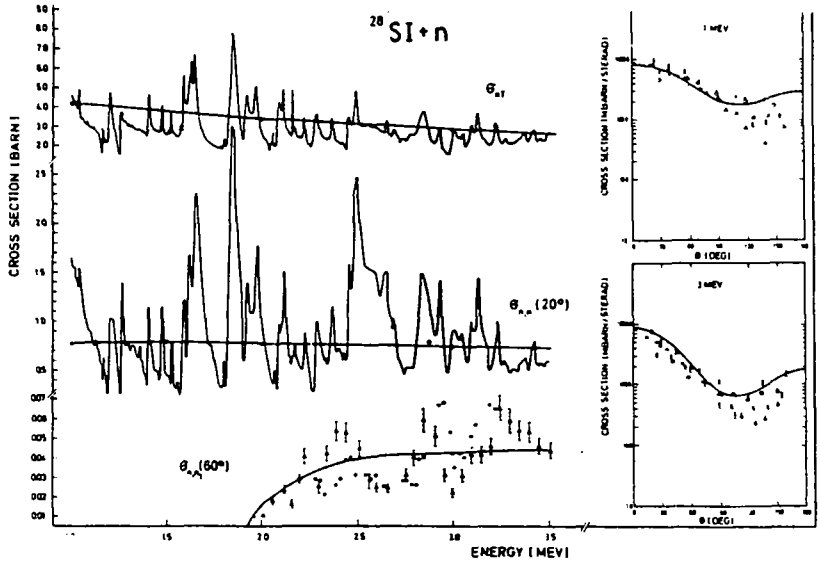

Fig. 9

i) the reality of level fluctuations seen in cross sections nearly the reaction threshold

and

ii) the appearence of non-statistical effects at higher neutron incident energies.

We started the investigation of charged-particle reaction cross sections in terms of the Hauser-Feshbach-formalism by testing the optical potential parameters for ^{28}Si+n recommended by several authors. A systematical analysis /23/ prooved a slightly changed potential obtained by Obst /24/ to be the best for a consistent description of neutron total cross section and elastic scattering angular distribution simultaneously within a wide range of neutron incident energies from about 2 up to 26 MeV. Other parameters involved in statistical model calculations have been taken from Perey's compilation of optical potentials /25/ and evaluated level schemes /26/, binding energies /27/ and nuclear level densities /28/ which are compiled in table 1.

The highly resolved level structure of the residual nuclei ^{28}Si, ^{28}Al, ^{27}Al and ^{25}Mg makes the application of the Hauser-Feshbach-model favourable but no computer code can handle such a

lot of decay channels. Using the code ELIESE-III /29/ a restriction to 31 channels at maximum holds. However, the number of levels in each decay mode should be choosen carefully to yield the lowest systematical error arising from an approximative determination of the Hauser-Feshbach-denominator. Clearly the absolute calculation of excitation functions of any particle transition must be cuted off at a definite excitation energy. Normally this energy cut-off is in the order of 10 MeV. Above this energy ELIESE-III can account for the competition of other decay channels by use of a nuclear level density distribution normally matched to the discrete level structure of that residual nucleus giving the most important contribution to the normalization factor (Hauser-Feshbach-denominator). This concept of an extension of the Hauser-Feshbach-formalism breaks down totally if any multi-particle emission channels will be opened. Considering Q-values of (n,n'p) or (n,n'α) the one-step-formalism is restricted to at least 15 MeV neutrons.

On the other hand, the energy range from 15 to 20 MeV is of great interest because data have been demanded but only scarce experiments were carried out. Therefore the extension of the applied statistical formalism is indispensable necessary to higher excitation energies including multi-step-processes and nuclear level continua in each residual nucleus formed in any cascade of particle emission. This advantage can be gotten under pain of angular distribution informations within the deexcitation mode. Several computer codes have been elaborated basing on that concept. The well-known code STAPRE /30/ has been used in this paper.

If here angular distributions are given for particle transitions to the first few excited states of a residual nucleus the following re-adjustment procedure has been applied:

i) calculation by ELIESE-III throughout the energy range up to 20 MeV;

ii) re-normalization of calculated angular distributions according to integral cross sections obtained by STAPRE if there are any differences in integral results.

An other problem connected with this extension of the statistical model should be pointed out here concerning the use of different nuclear level density formalisms. The success of the application of one or another formula has been discussed in several papers /31/ and depends strongly on the nucleus considered and the level density parameters taken from any compilation.

In the code STAPRE there has been implemented the so-called back-shifted-Fermi-gas-model. The application of this approach is supported by an excellent compilation of level density parameters $\underline{a}$ and the related parameters for the back-shift Δ and moment of inertia Θ /32/ for nuclear masses above $A > 28$. So in the mass range under investigation here ($24 \leq A \leq 29$) level density parameters and the corresponding quantities had been adjusted partially to fit the experimental data to a better extend. The parameters used have been compiled in table 2.

Basing on this method discussed above partial excitation functions of the first 8 low-lying levels in ^{28}Al as well as their angular distributions have been calculated. No adjustment must be applied besides the re-normalization of angular distributions at neutron incident energies higher than 10 MeV. Simultaneously the spectra of proton transitions to the level continuum in ^{28}Al were obtained yielding the total excitation function for ^{28}Si(n,p)^{28} Al also. Some results are shown in figs. 4 to 8.

3.2.2. Direct reaction contributions

Although the experimental information is insufficient to draw any definite conclusions on the appearence of non-statistical effects in ^{28}Si(n,p) reaction some indications for an influence there are. As mentioned above an irregularity in the angular

distribution (see figs. 6 and 7) is not explicable by the statistical model only. Furthermore, an enhancement of some proton transitions has been observed experimentally at 21.6 MeV /20/ corresponding to the excitation of the analogue of the giant dipole state in ^{28}Si both in position and magnitude (see fig. 8).

Up to now two authors /33, 34/ have tried to explain this deviations by taking into account a direct-reaction component. Best approach at 14 MeV was achieved in terms of a Finite-Range-DWBA (FR-DWBA) method using an effective n-p interaction assuming a Majorana exchange force with a Yukawa potential form factor /33/

$$V_{np} = P_M \, V(r) = P_M \, U_o \, \frac{\exp(-\mu r)}{\mu r}$$

with $U_o = 90$ MeV and $\mu^{-1} = 1.43$ fm.

It turns out that the value U_o needed to get reasonable agreement with experiments is larger by a factor of two than the one determined from the free n-p interaction usually. PWBA calculations yield incorrect results by an overestimation of cross sections. Also Zero-Range-DWBA approximations (ZR-DWBA) give worse results reflecting the fact that knock-out reactions are much more sensitive against finite-range effects than other direct reactions /34/.

Analogous calculations in terms of the FR-DWBA using same n-p interaction parameters have not been reported at other energies than 14 MeV. Results published by Liu et al. /34/ at 17 and 20 MeV cannot be taken for comparison because other exchange admixtures were applied.

Unfortunatly an appropriate computer code is not available to carry out FR-DWBA knock-out calculations with special n-p interaction terms. For an estimation of the energy dependence of knock-out contributions to (n,p_0) and (n,p_1) the reaction me-

chanism has been simulated by a ZR-DWBA approach with interaction parameters taken from Agodi /33/. The calculations were carried out using the computer code DWUCK /35, 36/.

The neutron and proton orbitals have been assumed to be ($1d_{5/2}$, $1d_{5/2}$) and ($1d_{5/2}$, $1d_{3/2}$) for the ground state and the first excited state in ^{28}Al. The other parameters compiled in table 1 were applied. In reviewing the results obtained for the p_0 and p_1 group following conclusions can be drawn:

i) generally, the (n,p_1) cross sections are higher in magnitude than the (n,p_0) reaction (fig. 5);

ii) no other higher order proton transitions have been calculated because any comparison to experimental angular distributions is speculative by scarce data /15/.

iii) Adding a statistical reaction contribution of about 0.5 mb / sr to the absolutely calculated knock-out cross section for (n,p_0) and (n,p_1) at 14 MeV a consistent with experimental data description was achieved (fig. 7). This value is in good agreement with a contribution of 0.4 mb/sr found by Agodi /33/.

3.3. Comparison of experimental and theoretical results

Although clear evidence for direct reaction contributions at least for proton transitions leaving the residual nucleus ^{28}Al in the lowestlying states can be concluded from measurement /15/ these effects are far from being explained by nuclear theory consistently. The interpretation of angular distribution of p_0 and p_1 transitions at 14 MeV is very encouraging assuming an incoherent superposition of a statistical component and a direct knock-out reaction contribution. But no experiments are available at present giving any reliable substance for an extension of this formalism to other proton groups at energies above 14 MeV.

From the point of data accuracy achieved this may be a striking disadvantage. All data known can be well interpreted within the error limits in terms of the statistical model as can be seen in figs. 4 to 8. However, to improve our knowledge on direct (n,p) processes more accurate data should be aquisited.

Finally some conclusions concerning recommended data can be noted:

i) total excitation function $^{28}Si(n,p)^{28}Al$

Figure 4 demonstrates that recommended data by ENDF/B-IV and ENDL have been confirmed to be reliable. No significant changes must be applied. UKNDL and SAND-II evaluations should be excluded.

ii) partial excitation functions $^{28}Si(n,p_i)^{28}Al$

Only ENDF/B-IV recommends data of partial excitation functions for 15 transitions to resolved final states. From the experimental point of view, there is no real new evidence for a necessary change in the data included in ENDF/B-IV. Above roughly 18 MeV the data calculated by statistical model only should be used with caution because direct contributions may be considerable (fig. 5) at least for the transitions to lowest-lying levels in ^{28}Al. This results in an intercept of the steep descent of the excitation functions included in evaluations up to now.

iii) angular distributions of protons

Using the insufficient experimental data base it may be reasonable concluded the symmetry of angular distributions for proton transitions leaving the final nucleus in low-lying states at least up to an energy of about 10 MeV. Above 10 MeV more knowledge on the asymmetric behaviour of angular distributions should really be included in evaluated data files at least for p_0 and p_1 transitions. On the other hand, proton transitions leading to higher-excited states in ^{28}Al may be assumed to be isotropic in agreement with approaches commonly used.

iv) proton emission spectra from $^{28}Si+n$

The inclusion of proton spectra in evaluated data files may be proposed here. No evaluations are known but from theoretical points of view these data can be obtained with rather good confidence by statistical model calculations in the whole energy range taking into account protons from (n,pn) also (fig. 8).

v) (n,p) in natural Silicon

Considering the contributions of isotopes to natural Silicon (^{28}Si=92.21 %, ^{29}Si=4.70 %, ^{30}Si=3.09 %) and the corresponding Q-values of -3.85 MeV, -2.9 MeV and -7.7 MeV respectively it may be obviously seen that the total Si(n,p) cross sections are determined mainly by the isotope ^{28}Si within the limits of experiments and evaluations. In reply on partial excitation functions the situation is not so simple but normally contributions from proton transitions to resolved states in ^{29}Al and ^{30}Al will be neglected in total. In other case they must be estimated by nuclear theory only because of absence of any experimental result.

4. $^{28}Si(n,d)^{27}Al$

4.1. Review of experimental data base

Because informations are lacking the (n,d) reaction appears to be the one of most uncertain neutron-induced reaction in ^{28}Si. Only relative and very scarce experimental data exist for partial excitation functions (n,d_0) and (n,d_1+d_2) done by Bohne /37/ from 16 to 22 MeV (see figs. 10 and 11). Further, at 21.3 MeV a relative angular distribution measurement for first 6 deuteron groups has been obtained by these authors also. Bharut-Ram et al. /20/ reported on measured angular distributions of (n,d_0) and (n,d_1+d_2) giving point for normalization of angular distributions at 21.6 MeV (figs. 12 to 16).

No measurements are available on the total excitation function because the activation technique is not applicable by the reason

of stable residual nucleus ^{27}Al. Also total deuteron spectra havn't been obtained up to now because of the complexity of the emission spectra (see discussion in section 3.1.).

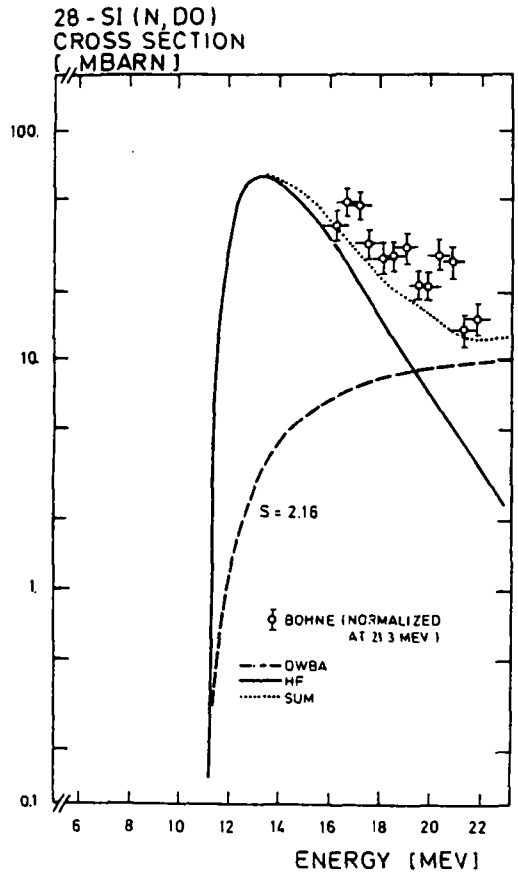

Fig. 10

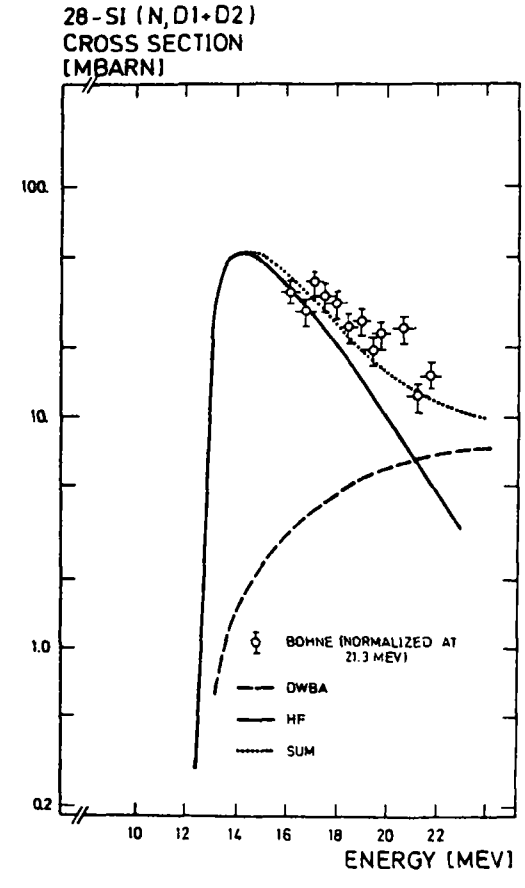

Fig. 11

So, in the most developed recommended data file ENDF/B-IV the total excitation function is included. The aim of this investigation is an elucidation of our knowledge of neutron-induced deuteron emission in Si.

Bohne's measurements /37/ may be normalized using the cross section of the (n,α_0) transition at 21.6 MeV to have a value of 2.3 ± 0.4 mb /20/. Such a value is really substantiated by absolute measurements as will be referred in section 5.1. A scaling factor of 0.0068 ± 0.0005 for angular distributions and 7.5 ± 0.5 for partial excitation functions can be deduced from this.

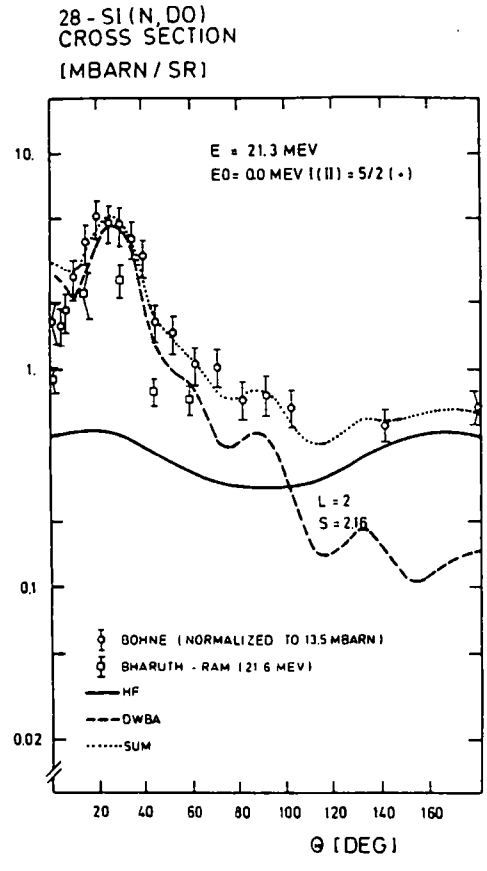
28-SI(N,D0)
CROSS SECTION
(MBARN/SR)
E = 21.3 MEV
E0= 0.0 MEV I(I) = 5/2(+)
L=2
S=2.16
BOHNE (NORMALIZED TO 13.5 MBARN)
BHARUTH-RAM (21.6 MEV)
HF
DWBA
SUM
10.
1.
0.1
0.02
20
40
60
80
100
120
140
160
Θ (DEG)

Fig. 12

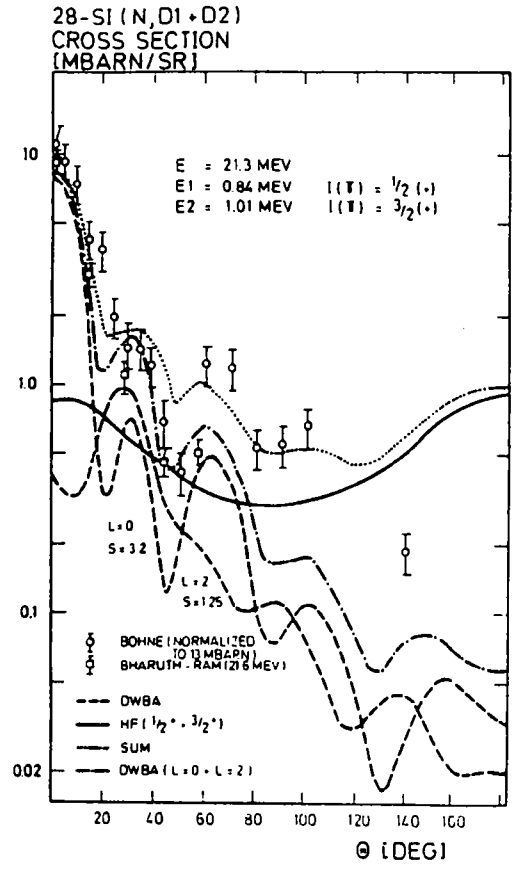
28-SI(N,D1+D2)
CROSS SECTION
(MBARN/SR)
E = 21.3 MEV
E1 = 0.84 MEV I(I) = 1/2(+)
E2 = 1.01 MEV I(I) = 3/2(+)
L=0
S=3.2
L=2
S=1.25
BOHNE (NORMALIZED TO 13 MBARN)
BHARUTH-RAM (21.6 MEV)
DWBA
HF (1/2+, 3/2+)
SUM
DWBA (L=0+L=2)
10
1.0
0.1
0.02
20
40
60
80
100
120
140
160
Θ (DEG)

Fig. 13

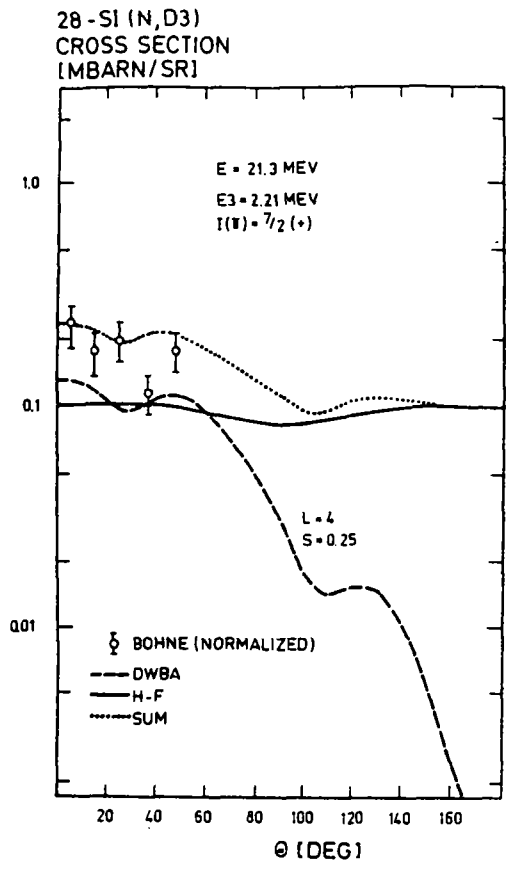

Fig. 14

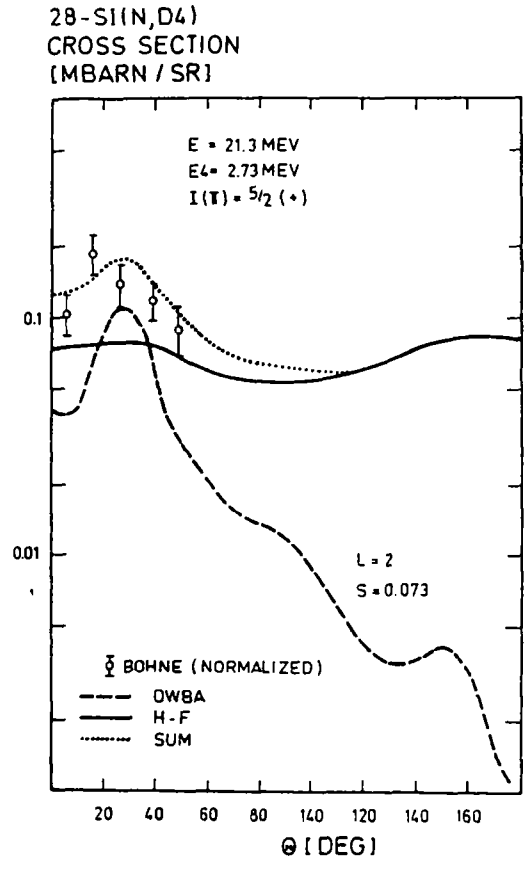

Fig. 15

In figs. 10 and 11 all normalized experimental informations on partial excitation functions have been summarized, whereas figs. 12 to 16 show angular distributions of several separated (or grouped) deuteron transitions leaving the residual nucleus ^{27}Al in the ground state or the lowest-lying excited states.

Fig. 16

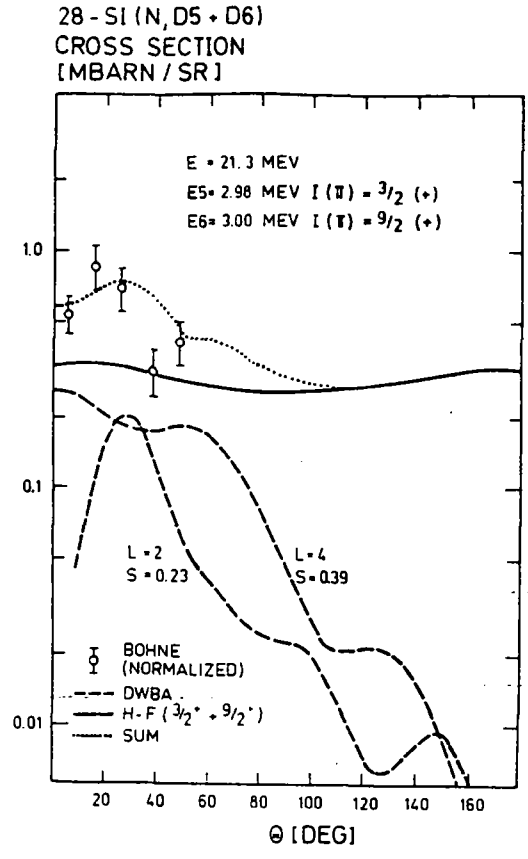

4.2. Interpretation of experimental data in terms of reaction model calculations

4.2.1. Statistical model application

Because of the very high Q-value of -9.36 MeV a simple application of the Hauser-Feshbach formalism is forbidden. ELIESE-III cannot handle such a lot of discrete levels to yield a correct normalization. To have an estimation of the statistical model prediction for deuteron angular distributions the α-decay channels had to be excluded in favour of deuteron transitions to low-lying states in ^{27}Al. This error should be corrected for by a re-adjustment (factor less than 1) afterwards. Angle-integrated cross sections for partial and total excitation functions

have been obtained applying the code STAPRE by a proper choice of nuclear level densities (see table 2) and a matching to ELIESE's results around 14 MeV.

All statistical model calculations have been included in figs. 10 to 16 demonstrating clearly that several transitions proceed via direct reaction mechanism mainly.

4.2.2. Interpretation of $^{28}Si(n,d)$ in terms of a p-pick-up process

It is a well-established fact that (nucleon, d) reactions proceed via a pick-up process taking a nucleon from the target nucleus. This mechanism is well understood in terms of DWBA formalism using a parameter depending on spin coupling conditions in the transition under investigation:

$$\sigma^{exp}_{n,d_i}(E,\vartheta) = S_i \, \sigma^{DWBA}_{n,d_i}(E,\vartheta).$$

These spectroscopic factors S_i may be extracted by fitting angular distributions of deuteron transitions between resolved states in the target and final nucleus. All calculations have been carried out by code DWUCK /35, 36/. Optical potentials compiled in table 1 were taken from Bohne /37/. In any case the analysis should start from other potentials than those applied in the statistical model investigation. Generally, a smaller imaginary well depth is the most striking feature of such direct reaction optical potentials.

By this way, experimental angular distributions for the first 6 deuteron transitions /37/ at 21.3 MeV have been analysed after a proper normalization relativ to the (n,α_0) cross section at 21.3 MeV. Of course, taking a small contribution from statistical reaction mechanism added incoherently slightly different spectroscopic factors can be extracted. For transitions to higher-lying states in ^{27}Al only a very limited angle range from 0^o to about 60^o is available for the fitting procedure.

Therefore, the values S_i found here may not be determined unambigously.
Comparing these results with calculated spectroscopic factors /38/ and with other ones deduced from different experiments /39, 40/ the general agreement is very fair.

The rather good DWBA approximations indicate a really small compound nucleus contribution for the lowest states in ^{27}Al, which will increase with decreasing energy of emitted deuterons as well as with neutron incident energies. This is shown in table 4.

Proceeding from this concept the parameters fixed at 21.3 MeV have been used to predict the direct reaction contributions to partial excitation functions and angular distributions.
A superposition of direct and statistical components of partial and differential data yields reasonable results for the excitation functions (n,d_0) and (n,d_1+d_2) (see figs. 10 and 11). This lookes like a consistency test of the parameters applied.

4.3. Conclusions from the theoretical interpretation of $^{28}Si(n,d)$ cross sections

Only a rather small data base is available for the analysis in terms of nuclear theory. Nevertheless, at least at 21.3 MeV a consistent picture of partial cross sections can be achieved. This is the starting point to predict a lot of unobserved data for $^{28}Si(n,d)$. This has been done in the present work leading to following recommendations:

i) total excitation function $^{28}Si(n,d)^{27}Al$

is shown in fig. 17 and should be quoted especially because of the important deviations from other evaluations.

Fig. 17

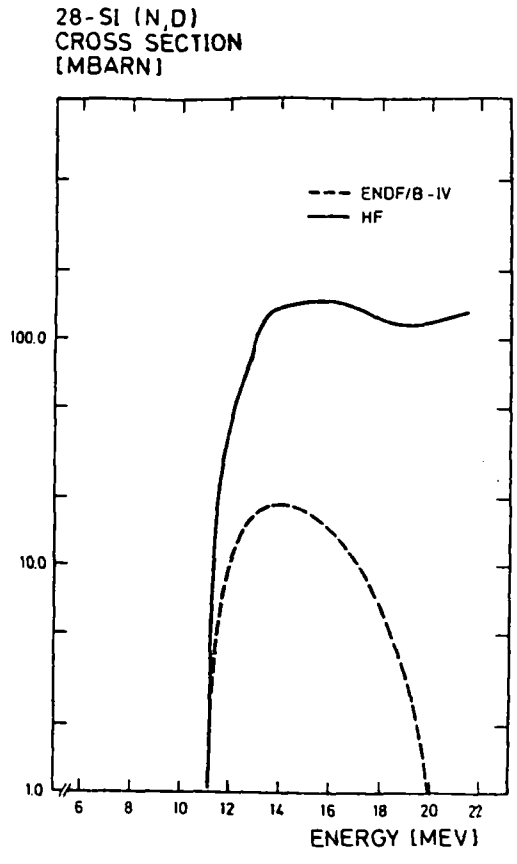

ii) partial excitation functions $^{28}Si(n,d_i)^{27}Al$

have been calculated up to the sixth deuteron group. No other data have been recommended up to now in any evaluated data file.

iii) angular distributions of deuterons

as is shown in figs. 12 to 16 strongly asymmetric angular distributions for the lowest deuteron groups can be expected. With increasing excitation energy of the final state the angular dependences will be more symmetric and isotropic finally. Calculations have been carried out for the first time in the present work.

iv) deuteron spectra from $^{28}Si+n$

have been calculated for deuteron transitions to the level continuum in the residual nucleus ^{27}Al. No comparison with experiments and other evaluations can be done.

v) (n,d) cross sections in natural Silicon

The reaction thresholds for ^{29}Si (n,d) (Q=-10.1 MeV) and ^{30}Si(n,d) (Q=-11.3 MeV) guarantee that the Si(n,d) cross sections may be mainly determined by the reactions on the isotope ^{28}Si within the confidence of all experiments and methods known at present.

5. Si(n,α)

5.1. Review of the experimental data base

To evaluate Si(n,α) cross sections contributions from $^{28}Si(n,\alpha)$ may be the most important ones but, because of the very low threshold of -0.036 MeV the $^{29}Si(n,\alpha)^{24}Mg$ reaction should be taken into account up to neutron energies of about 6 MeV at least. Therefore, in this paper $^{28}Si(n,\alpha)$ and $^{29}Si(n,\alpha)$ had been studied simultaneously.

Preliminary results for $^{28}Si(n,\alpha)$ have been reviewed formerly /41/. Referring to this publication the experimental data base may be characterized as follows:

i) scarce informations on the total $^{28}Si(n,\alpha)$ excitation function above 7 MeV because of unknown contributions from α-particle transitions leading to highly excited states in ^{25}Mg (see fig. 18).
The activation method can't be applied. Therefore all measurements /42 to 45/ are basing on α-particle spectroscopy.
A value of the (n,α)-systematics at 14 MeV has also been included /46/.

ii) rather good knowledge on partial excitation functions for the population of the lowest five final states in ^{25}Mg in the energy range of interest (see figs. 19 to 23).
Several authors had obtained absolute data in a wide energy range and with high energy resolution /42, 43, 47, 48, 49, 50, 51/.

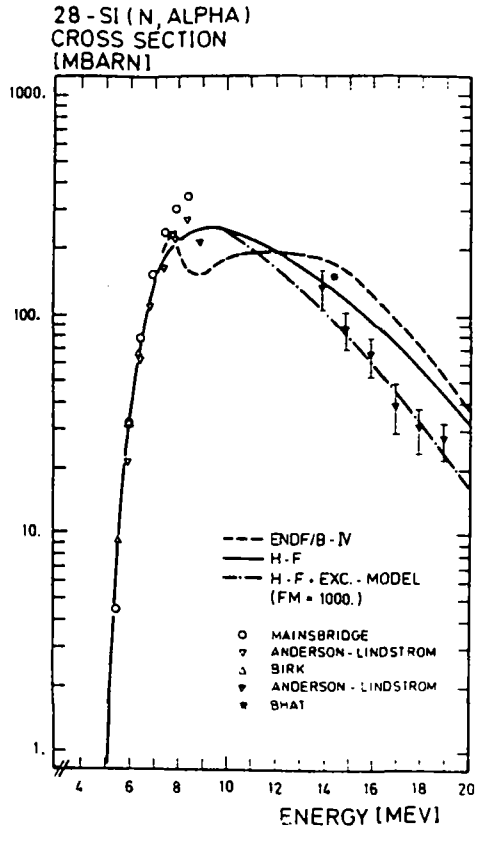

Fig. 18

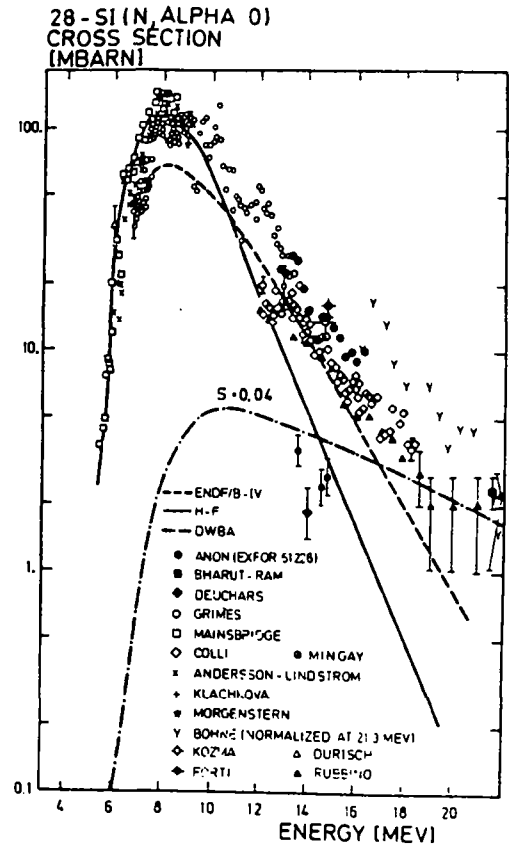

Fig. 19

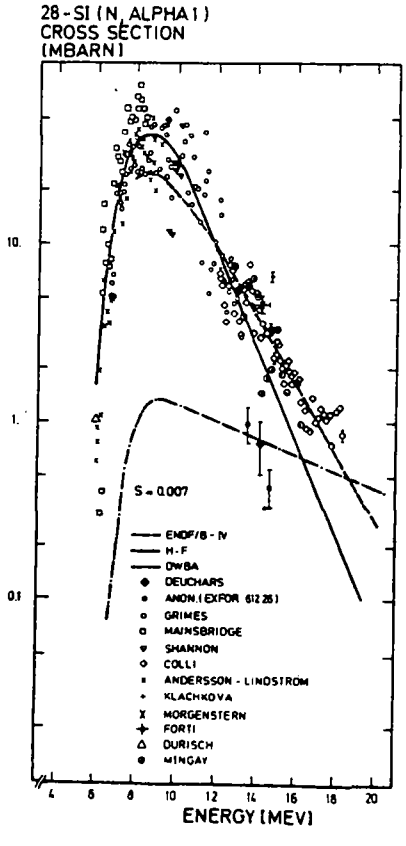

Fig. 20

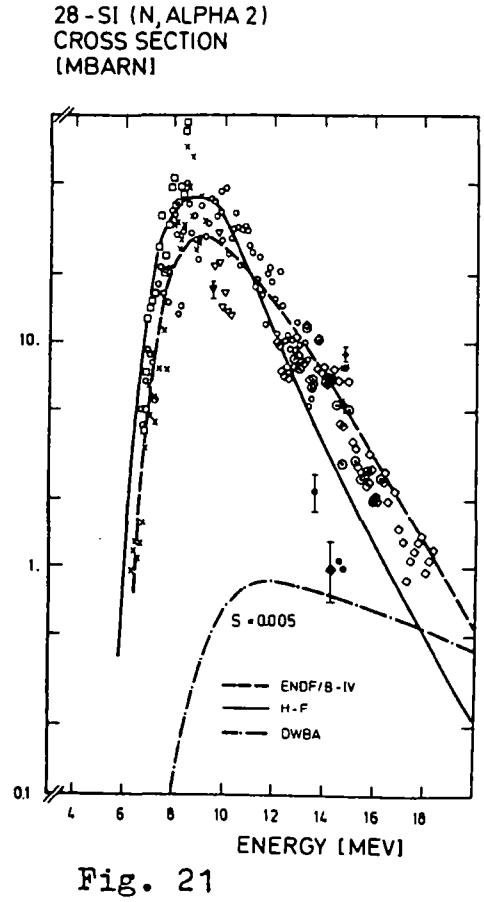

Fig. 21

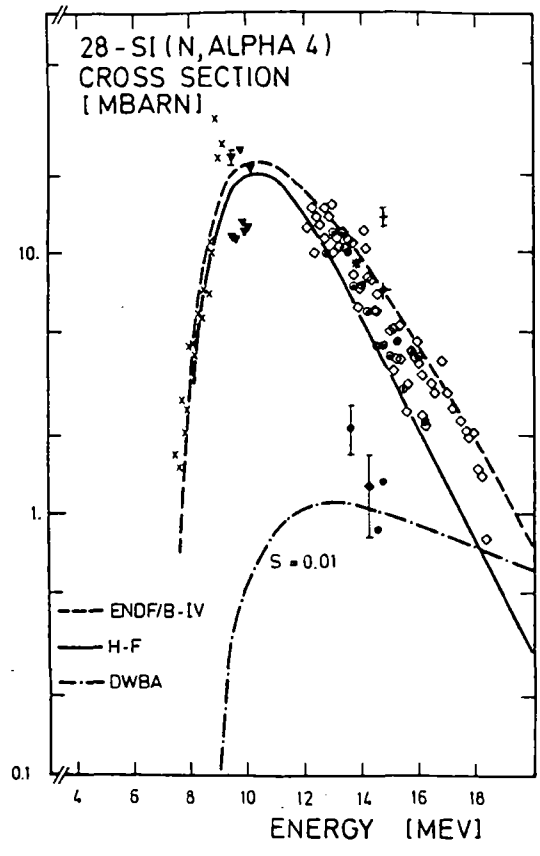

Fig. 22

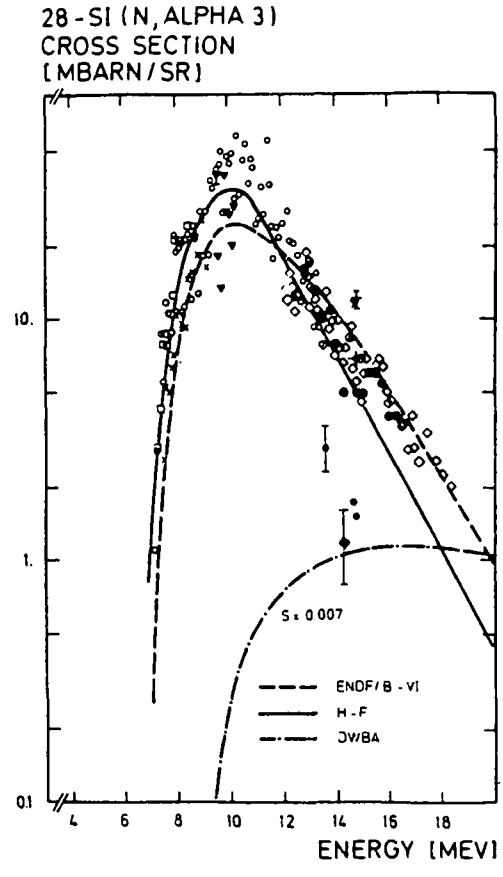

Fig. 23

The typical fluctuating structure in the excitation functions can be seen originating from an intermediate level structure in ^{29}Si.

In other cases single data points have also been used obtained from /15, 20, 52, 53, 54, 55, 56/. They have been included in the present analysis with only two exceptions /55, 56/ because of stringent deviations from a nearly consistent data base. In this frame also relative measurements published by Bohne /37/ for $^{28}Si(n,\alpha_0)$ could be normalized with high degree of confidence.

iii) scarce and contradictory experimental results on angular distributions of the first few α-particle groups at 14 MeV /15, 16, 54, 57/ (figs. 24 to 27) and for $^{28}Si(n,\alpha_0)$ at 21.3 MeV /37/ shown in fig. 28.

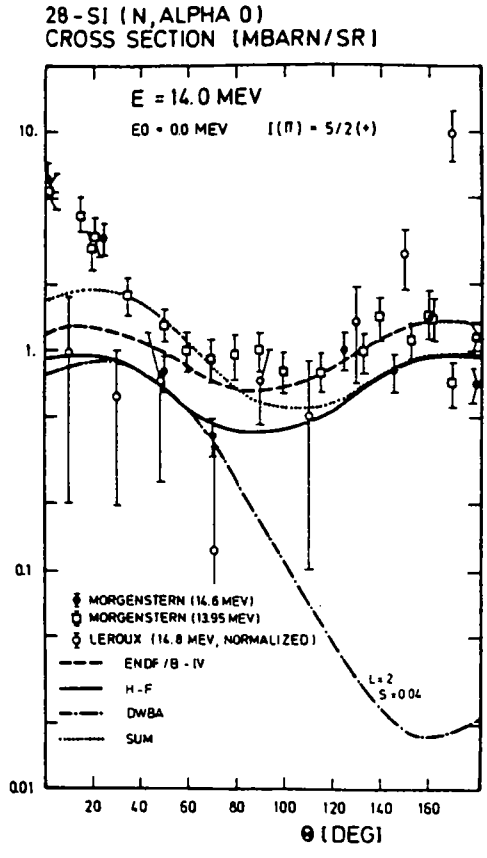

Fig. 24

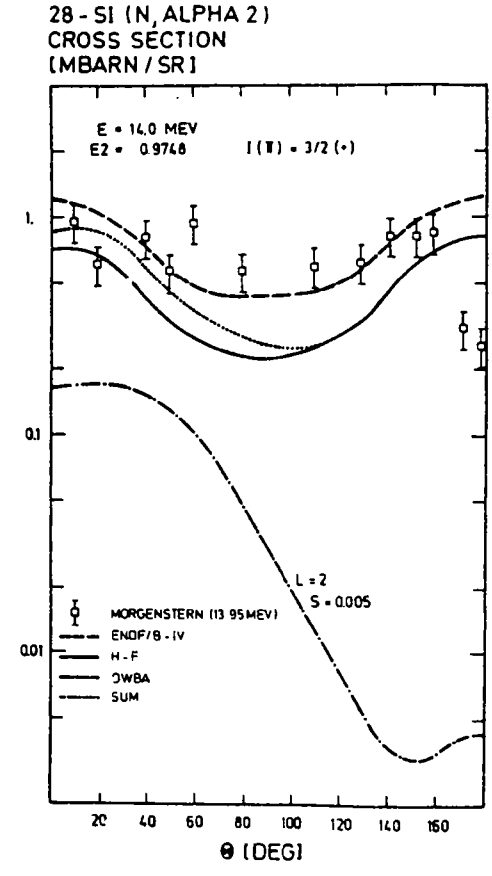

Fig. 25

Fig. 26

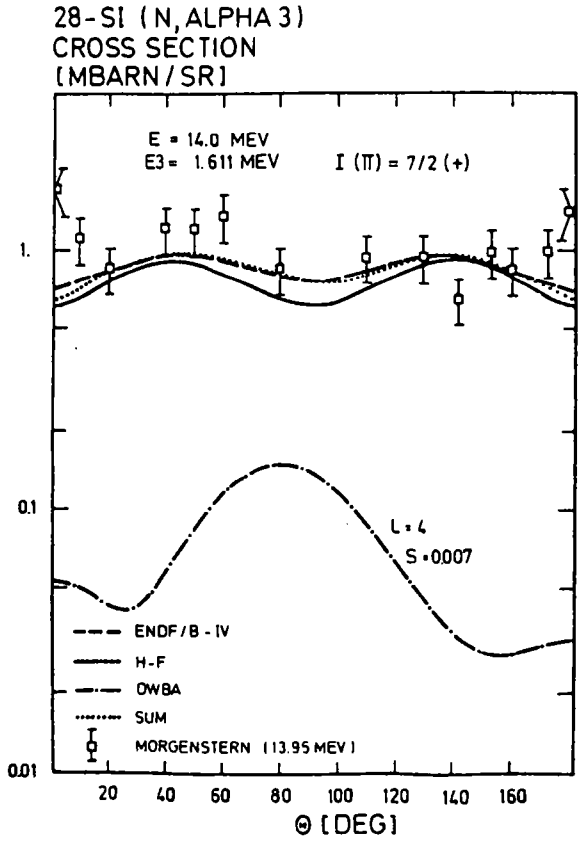

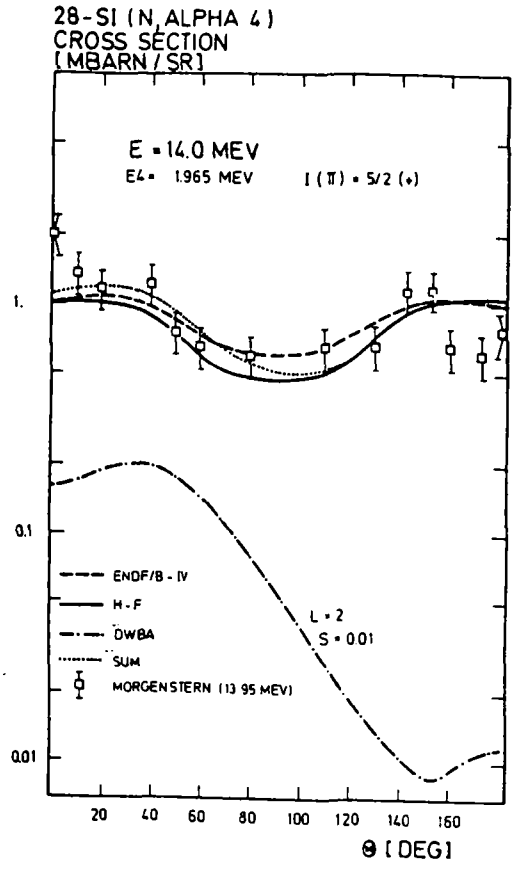

Fig. 27

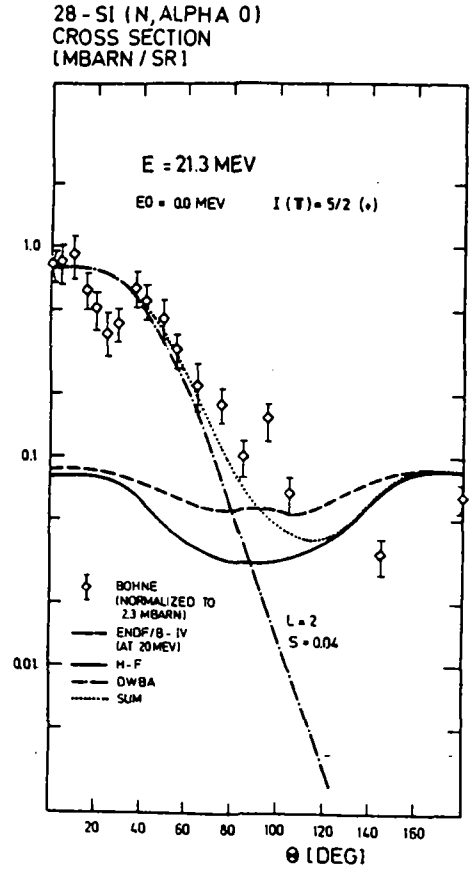

Fig. 28

iv) no reliable α-particle spectra can be obtained. Only one experiment at 14 MeV /54/ shown in fig. 29 in an absolute scale has been published. In several papers relative spectra in an unnormalizable scale (counts per channel) have been cited /49, 58/.

If we are looking for $^{29}Si(n,\alpha_1)^{26}Mg$ reactions and their relative contribution to a "sub-threshold" cross section background we must rake into account the excitation functions $^{29}Si\ (n,\alpha_0)$ and $^{29}Si(n,\alpha_1)$ at least. Searching the relevant data a reasonable amount of experimental informations can be found.

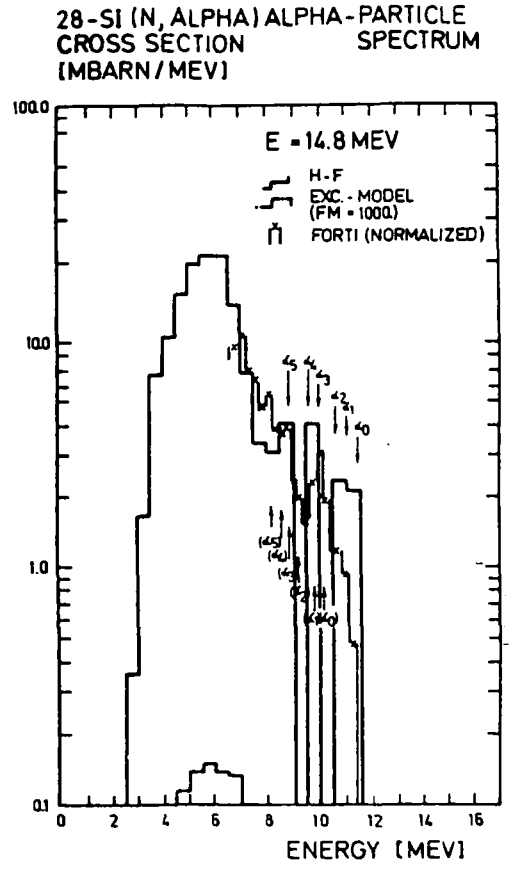

Fig. 29

By the reason that ^{26}Mg is also a stable nucleus only direct measurements using α-particle spectroscopy may be applied. The partial excitation function $^{29}Si(n,\alpha_0)$ is fairly well established from threshold up to 20 MeV by several experimentalists /50, 51, 52, 58, 59, 60, 61/ (see fig. 30). In good agreement an intermediate structure seen in the excitation functions is reproduced by several authors /42, 59, 60, 62, 63/. Such structures arise from a relatively low nuclear level density in ^{30}Si in this range of excitation energy under consideration. An estimation at 14 MeV excitation energy yields a value of $\langle \Gamma \rangle \approx 10$ keV and $\langle D \rangle \approx 50$ keV /59/.

From this difficulties in the theoretical interpretation of experimental data can be expected.

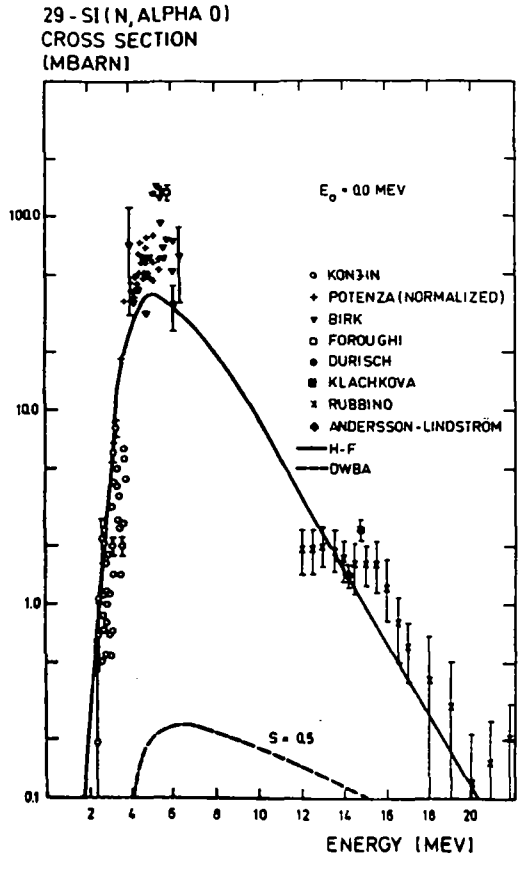

Fig. 30

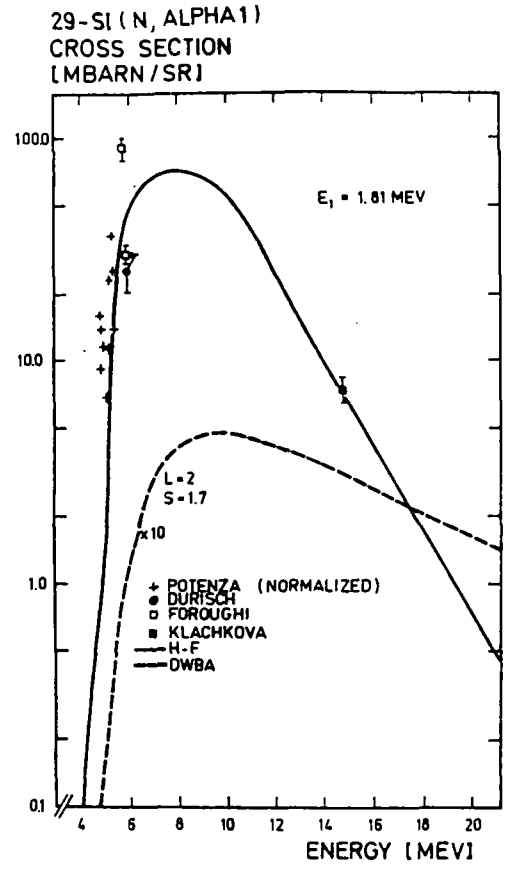

Fig. 31

Only a few data are available on $^{29}Si(n,\alpha_1)$ partial cross section (fig. 31). Absolute data obtained by /51, 52, 61/ must be combined with re-normalized relative measurements from /42, 63/ applying scaling factors derived from the normalization procedure in (n,α_0) cross sections. Partial cross sections for α-particle transitions to higher excited states in ^{26}Mg have not been reported elsewhere.

Extremly incomplete experience we have on α-particle angular distributions also. There exist only measurements for $^{29}Si(n,\alpha_0)$ and (n,α_1) at 5.85 MeV by Foroughi /61/ (figs. 32 and 33). The data show strong forward peaked asymmetric distributions which are in disagreement with general trends observed in $^{28}Si(n,\alpha_0)$ and (n,α_1) at least at this low neutron incident energy (compare figs. 24 and 25).

So it seems necessary to apply nuclear theory to clear this confusing situation.

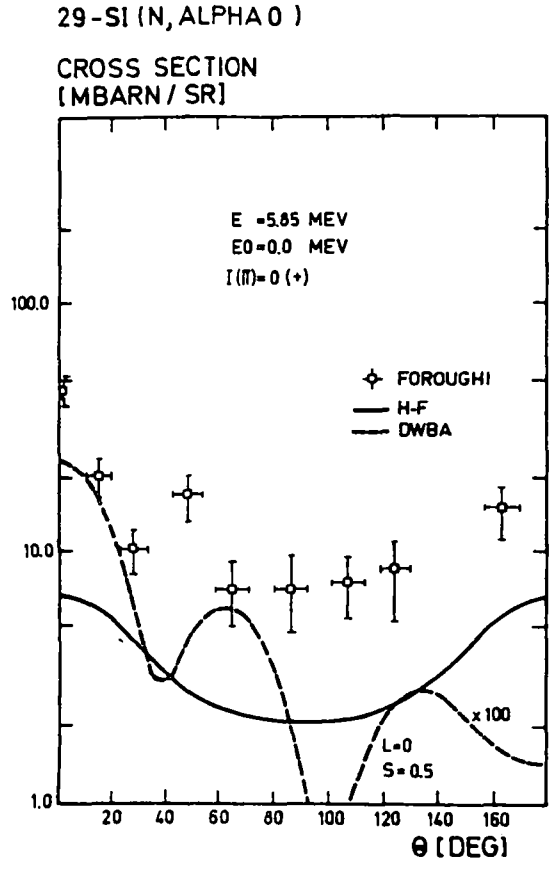

Fig. 32

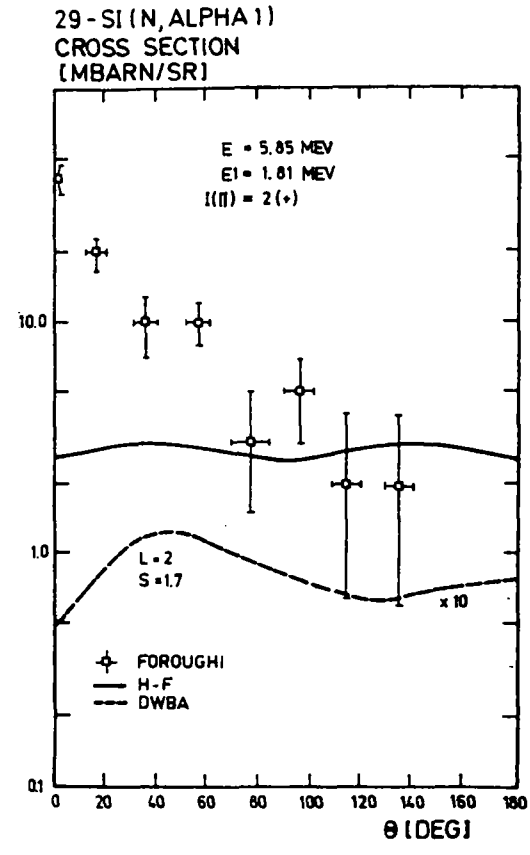

Fig. 33

5.2. Theoretical investigation of (n,α) processes in ^{28}Si and ^{29}Si

5.2.1. Statistical model calculations

In both target nuclei the (n,α_0)-threshold is low enough to have to taken a reasonable part of the level schema of the residual nuclei into account. So all calculations done by the code ELIESE-III are reliable up to an energy in the order of 10 MeV without any adjustment using parameters compiled in tables 1. Above that energy statistical model calculations have been continued by STAPRE adjusting level density parameters (table 2) and matching the results for partial excitation functions at about 10 MeV.

By such a method partial excitation functions for $^{28}Si(n,\alpha)$ and $^{29}Si(n,\alpha)$ have been obtained interpreting the experimental data base fairly well. Striking difficulties mainly arise from two aspects:

i) derivation of smooth experimental data from an averaging over the intermediate structure of the excitation functions;

ii) contributions from other than compound nuclear reaction mechanisms to excitation functions and angular distributions.

For both, examples will demonstrate that

i) it will never be possible to confirm Foroughi's measurements /61/ of $^{29}Si(n,\alpha_0)$ cross sections in absolute magnitude. The experiments are greater by a factor of roughly 3.8 also seen in the angular distribution (fig. 32);

ii) at high neutron incident energies the partial excitation functions show tails (figs. 19 to 23) and the angular distributions indicate also the appearence of direct reaction contributions (fig. 27) clearly.

5.2.2. Direct reaction model calculations

Previous studies of direct reaction contributions to (n,α) reaction on ^{28}Si start from knock-on processes /64/ or heavy-particle-stripping /65/ to explain a backward peaked angular distribution found experimentally by two authors /54, 57/ at 14 MeV using nuclear emulsion techniques. Later on, in contradiction to those measurements more recent experiments give strong evidence for foreward peaked angular distributions /15, 37/.

Following a systematics reviewed by Turkiewicz /66/ the medium weight nucleus Si should exhibit direct reaction modes proceed via a pick-up process of ^3He-clusters. To investigate such a direct reaction calculations have been done in a zero-range-DWBA (ZRDWBA) using the code DWUCK /35, 36/.

As most problematic point the choice of optical potentials in the entrance and exit channels has turned out influencing strongly the structure and normalization of angular distributions. Well established potential parameters compiled in table 1 have been used. The bound state wave functions for the ^{3}He-cluster were calculated as eigenfunctions of a real Woods-Saxon potential well with a depth adjusted to fit the separation energy of ^{3}He from target nucleus.

Superimposing the statistical component and the normalized by a factor direct reaction contribution angular distributions of α-particles leading to the ground state of ^{25}Mg as well as the first four excited states in ^{25}Mg have been calculated. The fitted spectroscopic factors are compiled in table 5. No other comparable spectroscopic factors concerning the $^{28}Si(n,\alpha)^{25}Mg$ reaction are known from experiment or theory.

An analogous procedure could not be carried out for $^{29}Si(n,\alpha)^{26}Mg$ because of the insufficient data base available at present. Therefore spectroscopic factors calculated by Meurders /38/ for the reaction $^{26}Mg(p,d)^{25}Mg$ have been adopted and used for comparison. The application of these values yield results which don't violate the experimental data as well as the principles of fundamental understanding of physics (see table 6).

From this point of view the suspect is hardened against strongly forward-peaked angular distributions found by some authors at lower neutron incident energies /15, 161/. Also old measurements yielding a pronounced backward scattering of α-particles /54, 57/ should be deleted by the same arguments. Further evidence for this decision comes from an really independent investigation concerning the profiles of (n,α) lines observed in Si-detectors irradiated with fast neutrons /67/ also indicating forward-peaked angular distributions.

Finally it should be stated that a study of $Si(n,\alpha)$ reaction in terms of knock-out mechanism may be interesting for further elucidation of the data base.

5.3. Conclusions for cross section recommendations of Si(n,α)

All data compiled and interpreted in the present paper will be compared to the best and most comprehensive recommended data file available at present (ENDF/B-IV, file 1194).

Following results had been found for:

i) total excitation function Si(n,α)

a remarkable lowering of (n,α) cross sections above 10 MeV in comparison to ENDF/B (fig. 18).

ii) partial excitation functions Si(n,α_i)

small corrections may be indicated for ^{28}Si(n,α_0) (fig. 19). Partial excitation functions of the first three α-particle groups of ^{29}Si(n,α_i) weighted according to the relative amount of ^{29}Si to the natural Silicon have been added.

iii) angular distributions of α-particles

above 15 MeV all angular distributions of α-particle transitions to the lowest-lying excited states in ^{25}Mg exhibit clearly asymmetric components which should be corrected for in MAT 1194. This effect is really smaller in ^{26}Mg understandable also from nuclear structure points of view.

iv) α-particle spectra

can be calculated to a reasonable accuracy by the statistical model and should therefore be included in recommended nuclear data files for use in near term future. Comparing theoretical results with experimental ones obtained at 14 MeV by Forti /54/ a significant shift in the calibration of α-particle energy scale can be seen (fig. 29). A wrong assignment of α-groups may be the reason for Forti's observation of backward-peaked angular distributions of the α-groups from α_0 to α_4.

v) cross sections for natural Silicon

may be the same as for $^{28}Si(n,\alpha)$ within the limits of confidence of evaluation methods with only the exception of a small "background" contribution below 6 MeV resulting from excitation functions $^{29}Si(n,\alpha_0)$ and $^{29}Si(n,\alpha_1)$ weighted according their amount to the natural isotopic composition.

6. Evaluation of other gas-production cross sections in Si

6.1. Si(n,t) and Si(n,^{3}He) reactions

6.1.1. Review of experimental data base

The argument that exotic reactions may be small enough to be negligable holds true for not too light nuclei only.

Although the experimental techniques have been developed during the past years, however, the reactions studied here are relatively difficult to measure /68/. Generally, informations can be found from systematics and phenomenological formulae describing data trends and isotopic effects in terms of an asymmetry parameter (N-Z)/A mainly in the mass range $A > 30$ and for atomic numbers $Z > 20$.

So, in the case of ^{28}Si a simple extrapolation to a asymmetry parameter value 0.0 will yield doubtful results.

Using such formulae reported by Qaim /68/ for (n,t) and (n,^{3}He) at 14.6 MeV following values can be estimated for ^{28}Si:

$$\sigma_{n,t}(14.6\ \text{MeV}) \approx 0.074\ \text{mb}$$

and

$$\sigma_{n,^3He}(14.6\ \text{MeV}) \approx 0.0088\ \text{mb}.$$

Studies of these reactions at an averaged neutron incident energy of about 30 MeV (produced by 53 MeV-Deuteron break up on ^9Be-targets) carried out by Qaim also /69/ using tritium counting techniques yields

$$\sigma_{n,t}(30\ \text{MeV}) \approx (3.5 \pm 1)\ \text{mb}.$$

Recently measurements on the (n,^{3}He) reaction at high incident neutron energies have been done by Qaim /70/ giving a ^{3}He to ^{4}He emission cross section ratio in dependence on the target atomic number. For Z=14 a value of

$$\sigma_{n,\,^3He}(30\ MeV) = 0.075\ \sigma_{n,\alpha}(30\ MeV)$$

can be deduced.

The experimental situation is compiled in fig. 34.

Fig. 34

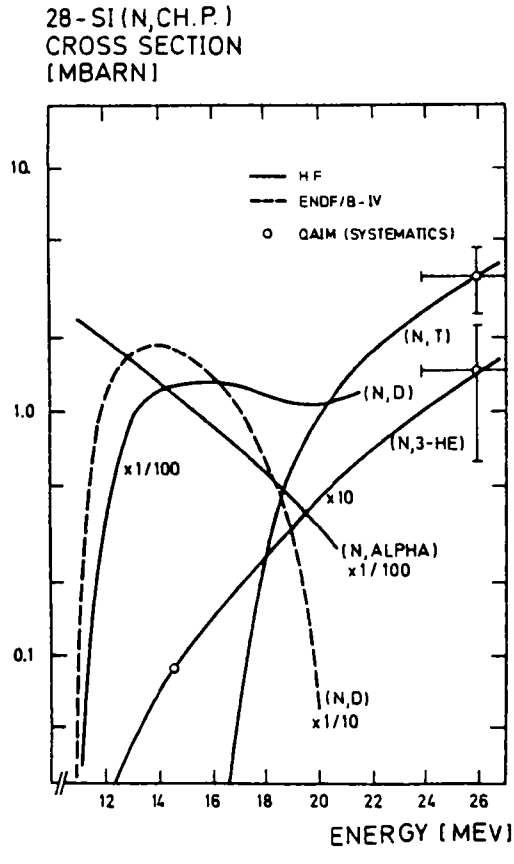

6.1.2. Reaction model predictions

The mechanisms of neutron induced (n,t) and (n,^{3}He) reaction in the medium mass region are as yet not well understood. From angular distributions of tritons emitted in (n,t) on light mass nuclei could be shown that this reaction proceeds via a direct reaction mechanism like a deuteron-pick-up.

The very small cross section arise from the competition between an emission of a bound triton which is less favoured than the emission of three unbound nucleons.

From the observation of the ratio of ^{3}He relative to ^{4}He emission /70/ a favoured emission of a bound ^{3}He-particle over the emission of three single nucleons may be indicated.

Therefore, both reactions may be assumed to show significant contributions from statistical model and direct mechanisms whi are increasing with increasing neutron incident energy. Unfortunatly, no angular distribution is available for a study of the situation discussed. Further also no well-established triton and ^{3}He optical potential parameters in the mass and excitation energy range needed here could be found /25/. From these aspects no model calculations have been done neither in the Hauser-Feshbach model nor in any sophisticated particle-transfer model for Si in the present work. On the other hand, calculations of the excitation functions of $^{28}Si(n,^{3}He)$ and $^{27}Al(n,t)$ were done by Qaim et al. /71/ in terms of statistical model only.

The recommended data shown in fig. 34 are basing on a speculative evaluation of scarce and uncertain informations.

6.2. Si(n,n'p) and Si(n,n'α) reactions

6.2.1. Review of experimental data base

It has been shown by Qaim /72/ that contributions of (n,n'p) and (n,n'α) reactions are not negligable at least above 14 MeV and attention should be given to this cross sections in gas-production calculations.

Measurements are difficult and using activation technique only the sum of (n,d) + (n,n'p) + (n,pn) can be obtained. On the other hand by a proton spectroscopy the observed proton spectra have to be convoluted by means of theoretical analysis of energy and angular distributions of the emitted protons. Therefore this method has not been applied so far.

Any information for Si can only be gotten from data systematics. At mass number A >30 the (n,d) cross section is small compared to the sum (n,d) + (n,n'p) + (n,pn). The ^{28}Si (n,d) reaction cross section at 14 MeV recommended in this paper fits well the systematics given in /68/ extrapolating to an asymmetry parameter (N-Z)/A=0. Unfortunately this systematics don't allow any decisive conclusion on the sum cross section at zero asymmetry but a value $\sigma_{n,n'p} + \sigma_{n,pn}$ in the order of 300 to 400 mb can be expected really at 14 MeV.

From other authors an estimated sum cross section $\sigma_{n,d+n'p+pn} \approx 700 \pm 30$ mb at 14.4 MeV is quoted /73/.

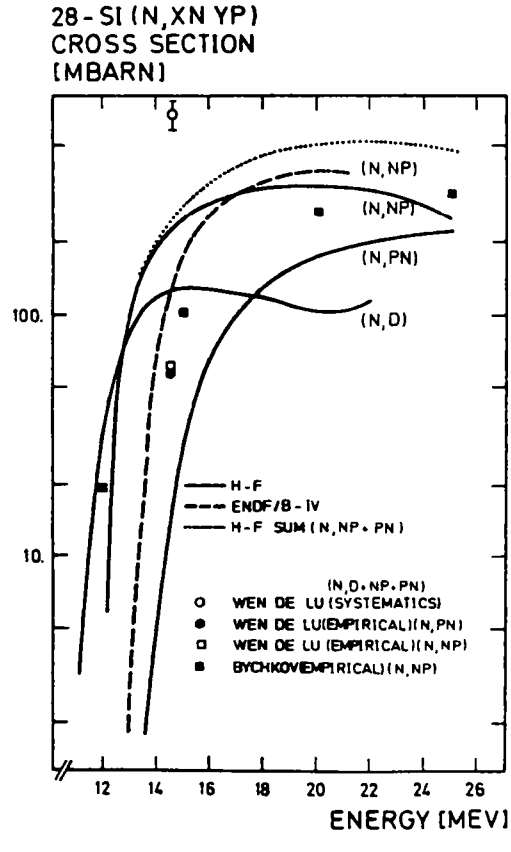

Fig. 35

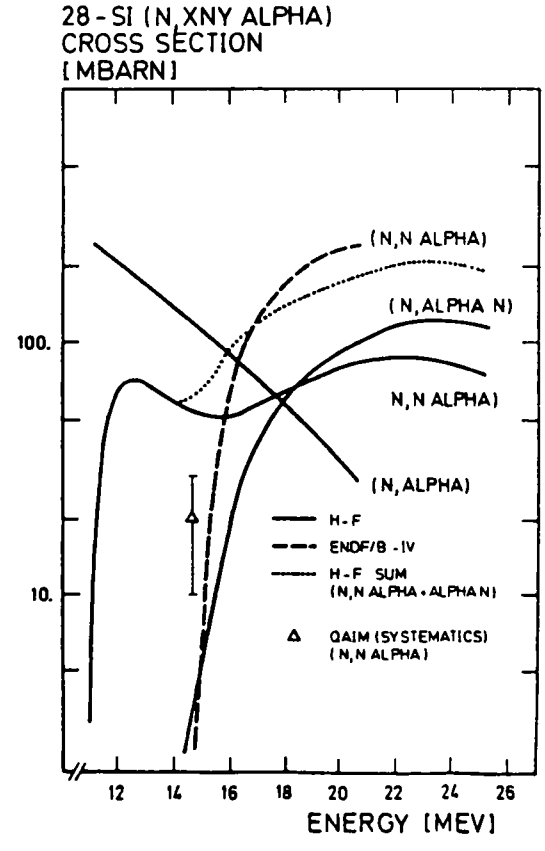

Fig. 36

As far as the (n,n'α) reaction is recommended the activation technique yields more reliable informations because contributions from different disturbing reactions (mainly (n,α)) can be

separated by radiochemical methods.

In the case of ^{28}Si no measurements can be carried out because of stable residual nuclei. So we have to rely upon systematics also for an estimate of $\sigma_{n,n'\alpha}$. Using a compilation given by Qaim /68/ a contribution of about 10 to 15 % of the (n,α) cross section at 14 MeV can be assumed to yield

$$\sigma_{n,n'\alpha}(14.7\ \text{MeV}) \approx 20\pm10\ \text{mb}.$$

All informations have been summarized in fig. 36. Most recently a preliminary result for total α-production cross section at 14.8 MeV has been reported /74/. The value of 218±11 mb compares reasonable well with our recommendation of about 184 mb.

6.2.2. Reaction model predictions

Although some systematical investigations have been made to calculate (n,n'p) cross sections using the statistical model incorporating precompound effects for medium masse nuclei /75/ any conclusion drawn from this to more light nuclei should be taken with caution.

The sequential emission of two or more nucleons in which one of them is a charged particle is not well understood at present. Generally, if the proton binding energy is smaller than that of the neutron the emission of protons is more probable than a neutron emission resulting in enhanced (n,n'p) cross section to the debit of (n,2n) processes. This should hold true especially in the ^{28}Si because of a very high (n,2n) threshold of Q=-17.2 MeV.

Calculations of (n,pn), (n,n'p), (n,αn) and (n,n'α) reaction cross sections were carried out using the code STAPRE. Results obtained may be, at all, speculative partly. Due to a total lack of experimental informations concerning excitation functions the adjustment of parameters is at least partially not substantiated by objective criteria.

The values given in figs. 35 and 36 may be regarded as recommendations basing on our best knowledge in nuclear data at present.

7. Summary

Our knowledge on cross sections for neutron-induced gas-production in Si is not very well established in all quantities from experiments and theoretical understanding.

On the other hand much more and more accurate data of these processes will be needed in future for fusion reactor material tests and other applied purposes.

Therefore, the present work was aimed to study the situation basing on most recent experiments and theoretical nuclear reaction models. A consistent interpretation of all informations could be achieved in most of the data quantities under investigation resulting in recommendations for the improvement of evaluated nuclear data files available for users.

Nevertheless, further investigations of low-yield nuclear reactions as well as angular distributions and spectra of emitted charged particles should be demanded with high priority.

Acknowledgment

The author wish to express his gratidude to Prof.Dr. D. Seeliger for his continuing interest in this work. Further Prof. Dr. R. Reif is thanked for valuable discussion of the results obtained in the frame of DWBA. Finally, Drs. B. Weißbach and R. Wolf will be acknowledged their support in using the codes DWUCK and CHUCK.

References

/1/ WRENDA 79/80, "World Request List for Nuclear Data", INDC(SEC)-73/URSF, Vienna 1979
WRENDA 81/82, INDC(SEC)-78/URSF, Vienna 1981

/2/ D. Hermsdorf, L. Neumann, Proc. IX. Int. Symp. on Interaction of Fast Neutrons with Nuclei, Gaußig 1979, ZfK-410, p. 147, 1980

/3/ J.M.F. Jeronymo, G.S. Mani, J. Olkowsky, A. Sadeghi, C.F. Williamson, Nucl. Phys. 47 (1963) 157

/4/ J.B. Marion et al., Phys. Rev. 101 (1956) 247

/5/ B. Mainsbridge et al., Nucl. Phys. 48 (1963) 83

/6/ M. Birk et al., Nucl. Instr. and Methods 21 (1963) 197

/7/ R. Bass et al., report EANDC(F) 66, 1966

/8/ A.V. Cohen et al., Nucl. Phys. 1 (1956) 73

/9/ B.D. Kern et al., Nucl. Phys. 10 (1959) 226

/10/ M. Bormann, in "Handbook on Nuclear Activation Cross Sections", Vienna, 1974

/11/ N. Ranakumar et al., Nucl. Phys. A122 (1968) 679

/12/ E.B. Paul et al., Can. Journ. Phys. 31 (1953) 267

/13/ J.E. Strain et al., report ORNL-3672, 1965

/14/ D.W. Mingay, J.P.F. Sell Shop, P.M. Johnson, Nucl. Instr. and Methods 94 (1971) 497

/15/ H. Morgenstern, D. Hilscher, J. Scheer, Nucl. Phys. 83 (1966) 369

/16/ H. Morgenstern, et al., Nucl. Instr. and Methods 39 (1966) 347

/17/ L. Colli et al., Nuovo Cim. 20 (1961) 928

/18/ W. Mausberg, Inst. für Kernphysik, Frankfurt/Main, report, IFK-14, 1965

/19/ K. Debertin, H. Günther, E. Rössle, Nucl. Phys. A101 (1967) 473

/20/ K. Bharut-Ram, S.M. Perez, F.D. Brooks, S.A.R. Wynchank, W.R.Mc Murray, Nucl. Phys. A278 (1977) 285

/21/ S. Cierjacks et al., report KFK-1000, 1969

/22/ I. Schouky, Thesis, Karlsruhe, 1979

/23/ L. Neumann, diploma work, TU Dresden, 1979, cited also in reference /2/

/24/ A.W. Obst, J.L. Weil, Phys. Rev. C7 (1973) 1076

/25/ C.M. Perey, F.G. Perey, At. Data and Nucl. Data Tables 17 (1976) 1

/26/ ENSDF-File, Version August 1978

/27/ P.M. Endt, C. van der Leun, Nucl. Phys. A310 (1978)

/28/ M. Beckermann, Nucl. Phys. A278 (1977) 333

/29/ S. Igarasi, report JAERI-1224, 1972

/30/ M. Uhl, B. Strohmaier, report IRK-01/76, 1976

/31/ V.A. Konshin, Nuclear Theory for Application, Proc. IAEA Trainings Course, Triest, 1980, IAEA-SMR-68/I, p.139,1981
V.A. Konshin, Proc. X^{th} Int. Symp. on Interaction of Fast Neutrons with Nuclei, Gaußig, 1979, ZfK-410, 1980, 141

/32/ W. Dilg, W. Schantl, H. Vonach, M. Uhl, Nucl. Phys. A217 (1973) 269

/33/ A. Agodi, G. Schiffrer, Nucl. Phys. 50 (1964) 337

/34/ K.H. Liu, E.V. Ivash, Nucl. Phys. A140 (1970) 444

/35/ P.D. Kunz, computer code DWUCK, unpublished

/36/ W. Dolak, H. Iwe, R. Wünsch, Annual report ZfK-243, 1972, 195

/37/ W. Bohne, D. Hilscher, H. Homeyer, H. Morgenstern, J.A. Scheer, Nucl. Phys. A111 (1968) 417

/38/ F. Meurders, P.W.M. Glaudemans, J.F.A. van Hienen, G.A. Timmer, Z. Physik A276 (1976) 113

/39/ H.E. Gove et al., Nucl. Phys. A116 (1968) 368

/40/ B.H. Wildenthal et al., Phys. Rev. 167 (1968) 1027

/41/ D. Hermsdorf, Proc. Xth Int. Symp. on Interaction of Fast Neutrons with Nuclei, Gaußig, 1980, ZfK-459 (1981) p. 158

/42/ B. Mainsbridge, T.W. Bonner, T.A. Rabson, Nucl. Phys. 48 (1963) 83

/43/ G. Andersson-Lindström et al., Soc. Roy. Science 10 (1964) 265

/44/ M. Birk et al., Nucl. Instr. and Methods 21 (1963) 197

/45/ G. Andersson-Lindström, Z. für Naturforschung 179 (1962) 238

/46/ M.R. Bhat et al., BNL-50379, 1973

/47/ P. Grimes et al., Nucl. Phys. A 124 (1969) 369

/48/ L. Colli et al., Nucl. Phys. 43 (1963) 529

/49/ R.G. Miller, R.W. Kavanage, Nucl. Instr. and Methods 48 (1967) 13

/50/ A. Rubbino, D. Zubke, Nucl. Phys. 85 (1966) 606

/51/ J.E. Durisch, F. Fouroghi, J. Rossel, Nucl. Instr. and Methods 52 (1967) 222

/52/ Klachkova et al., Atomn. Ehnerg. 42 (1977) 141

/53/ P. Kozma, P. Bém, J. Vincour, Proc. 2nd Symp. on Neutron-Induced Nuclear Reactions, Smolenice 1979, Physics and Applications Vol. 6, 1980, 113

/54/ P. Forti, E. Gadioli, A. Marini, Nuov. Cim. 41A (1966) 52

/55/ EXFOR entry 61226

/56/ Deuchars et al., Nature 191 (1961) 995

/57/ B. Leroux, J. Dalmas, Ph.Th. Doan, Ph.Le Thanh, R. Chastel, Nucl. Phys. 67 (1965) 333

/58/ G. Andersson-Lindström, Z. für Naturforschung 17a (1962) 238

/59/ J. Konjin, A. Lamber, Nucl. Phys. 48 (1963) 191

/60/ M. Birk, G. Goldring, P. Hillman, Nucl. Instr. and Methods 22 (1963) 197

/61/ F. Foroughi, J. Rossel, Helv. Phys. Acta 43 (1970) 432 and Helv. Phys. Acta 45 (1972) 439

/62/ Jaskola et al., Nucl. Phys. 79 (1966) 108

/63/ R. Potenza, R. Ricamo, A. Rubbino, Nucl. Phys. 41 (1963) 298

/64/ J.N. Massot, E. El-Baz, J. Lafoncriére, J. de Physique 26 (1965) 527

/65/ P. Forti, E. Gadioli, A. Marini, Nuov. Cim. B1 (1966) 244

/66/ J. Turkiewicz, Proc. 2nd Int. Symp. on Neutron-Induced Reactions, Smolenice, 1979, in Physics and Applications, Vol. 6, p. 13

/67/ G. Paić, K. Kadija, B. Ilijas, K. Kovacević, Nucl. Instr. and Methods 188 (1981) 119

/68/ S.M. Qaim, Proc. Int. Conf. on Neutron Physics and Nucl. Data for Reactors and other Applied Purposes, Harwell, 1978, p. 1088

/69/ S.M. Qaim, R. Wölfle, Nucl. Phys. A295 (1978) 150

/70/ C.H. Wu, R. Wölfle, S.M. Qaim, Nucl. Phys. A329 (1979) 63

/71/ S.M. Qaim, H.V. Klapdor, H. Reiss, Phys. Rev. C22 (1980) 1371
S.M. Qaim, R. Wölfle, H. Liskien, Phys. Rev. C25 (1982) 203

/72/ S.M. Qaim, G. Stöcklin, Cited in /68/

/73/ Wen-deh Lu, R.W. Fink, Phys. Rev. C4 (1971) 1173

/74/ D.W. Kneff, private communication , 1982

/75/ K. Seidel, D. Seeliger, A. Meister, Yad. Fiz. 23 (1976) 745

Table 1: Optical potential parameters used in the statistical model (SM) and DWBA calculations. The potential depth are in MeV, the diffuseness and radius parameter in fm. The potential form factors are of Woods-Saxon and Woods-Saxon derivative respectively.

Nucleus		real part			imaginary			spin-orbit part	references/ remarks
		V	r_v	a_v	W	r_w	a_w	V_{so}	
^{28}Si + n	SM	52.0	1.15	0.78	12.1	1.25	0.47	9.0	/24/
	DWBA	40.0	1.45	0,35	8.8	1.45	0,35	-	/34/(n,p)
		40.8	1.30	0.66	5.0	1.26	0.48	6.0	/37/(n,d)
		52.0	1.15	0.78	0.6 E	1.25	0.47	4.9	- (n,α)
^{28}Al + p	SM	52.0	1.15	0.78	12.1	1.25	0,47	9.0	/24/
	DWBA	40.4	1.45	0.19	9.2	1.45	0.19	-	/34/(n,p_o)
		40.4	1.45	0.19	8.2	1.45	0.19	-	/34/(n,p_1)
^{25}Mg + α	SM	51.2	1.694	0.585	11.13	1.694	0.585	-	/25/
	DWBA	51.2	1.694	0.585	8.8	1.694	0.585	-	/25/
^{27}Al + d	SM	84.0	1.25	0.77	6.2	1.28	0.65	6.0	/37/
	DWBA	84.0	1.25	0.77	6.2	1.28	0.65	6.0	/37/
^{29}Si + n	SM	52.0	1.15	0.78	12.1	1.25	0.47	9.0	/24/
	DWBA	52.0	1.15	0.78	0.6 E	1.25	0.47	9.0	/24/

^{24}Mg + α	SM	51.2 1.694 0.585	8.8 1.694 0.585	-	/25/
	DWBA	51.2 1.694 0.585	8.8 1.694 0.585	-	/25/

Table 2: Level density parameters used in statistical model code STAPRE ($\Theta = I_{eff}/I_{rigid}$)

Nucleus	a/ MeV^{-1}	Θ	Δ/ MeV	references
^{27}Si	4.5	1.0	-2.5	/23/, /32/
^{28}Si	4.0	1.0	+1.0	/23/, /32/
^{29}Si	3.5	1.0	+5.0	/28/
^{30}Si	3.5	1.0	+1.5	/28/
^{27}Al	3.0	1.0	-2.0	/28/
^{28}Al	4.0	1.0	-4.0	/23/, /32/
^{24}Mg	3.0	1.0	+2.0	/28/
^{25}Mg	4.5	1.0	-2.5	/23/, /32/

Table 3: Spectroscopic factors S deduced from proton-pick-up processes in ^{28}Si exciting lowest-lying states in ^{27}Al

Level no.	Excitation energy/MeV	I^{π}	$^{28}Si(n,d_i)^{27}Al$ S(absolute) this work	/38/	S (relative) this work	/37/	$^{28}Si(d,p_i)^{27}Al$ S (relative) /39/	/40/
0	0.0	$5/2^+$	2.16	5.5	1.0	1.0	1.0	1.0
1	0.8431	$1/2^+$	3.20	1.00	1.48	0.34	0.25	0.13
2	1.010	$3/2^+$	1.25	0.90	0.58	0.18	0.24	0.15
3	2.209	$7/2^+$	0.25	-	0.12	0.11	-	<0.11
4	2.732	$5/2^+$	0.073	1.1	0.033	0.034	0.24	0.16
5	2.980	$3/2^+$	0.23	~0.5	0.11	≤0.18	<0.08	≤0.1
6	3.001	$9/2^+$	0.39	-	0.18	≤0.11	-	≤0.16

Table 4: Direct reaction contributions to $^{28}Si(n,d_i)$ cross sections (in percents)

Neutron energy/MeV	deuteron group i						
	d_0	d_1	d_2	d_3	d_4	d_5	d_6
21.3	65	60	43	35	25	27	34

Table 5: Spectroscopic factors S deduced from ^3He-pick-up reaction calculations on ^{28}Si exciting the lowest-lying levels in ^{25}Mg

Level no.	Excitation energy/MeV	I^π	$^{28}Si(n,\alpha_i)^{25}Mg$ S (absolute) this work	/38/	S (relative) this work	/38/
0	0.0	$5/2^+$	0.04	2.0	1.0	1.0
1	0.59	$1/2^+$	0.007	0.11	0.175	0.055
2	0.97	$3/2^+$	0.005	0.08	0.125	0.04
3	1.61	$7/2^+$	0.007	-	0.175	-
4	1.91	$5/2^+$	0.01	0.15	0.25	0.075

Table 6: Direct reaction contributions to $^{28}Si(n,\alpha_i)$ and $^{29}Si(n,\alpha_i)$ cross sections (in percents)

Target nucleus	Neutron energy/MeV	α-particle group i					Model	Refe-rences
		α_0	α_1	α_2	α_3	α_4		
^{28}Si	~14	33	17	11	11	12	^{3}He-pick-up	this work
		65		49			Heary-part.-strip.	/65/
	21.3	78	-	-	-	-	^{3}He-pick-up	this work
^{29}Si	5.85	~0.5	~0.2	-	-	-	^{3}He-pick-up	this work

Figure captions

Fig. 1 Excitation function for Si(n,p). Comparison of evaluated data recommended by several neutron nuclear data libraries.

Fig. 2 Same as fig. 1 for Si(n,d).

Fig. 3 Same as fig. 1 for Si(n,α).

Fig. 4 Excitation function for ^{28}Si(n,p). Comparison of experimental data, evaluated data for ENDF/B-IV and calculated ones by the present work (H-F).

Fig. 5 Excitation function for ^{28}Si(n,p_0+p_1). Calculations by the present work (H-F and DWBA) are compared to experimental data and evaluated ones by ENDF/B-IV.

Fig. 6 Angular distributions of the proton groups p_0+p_1 from ^{28}Si(n,p) at about 9 MeV. Calculated results (H-F and DWBA) are compared to experimental ones.

Fig. 7 Same as fig. 6 at 14 MeV.

Fig. 8 Proton emission spectrum from Si(n,p) at 21.6 MeV neutron incident energy. Statistical model calculations (H-F) are compared with experimental ones.

Fig. 9 Resonance structure observed in Si+n total, elastic and inelastic scattering cross sections from 1 to 3.5 MeV. Experimental data obtained by Cierjacks /21/ (σ_{nT}), Schouky /22/ ($\sigma_{n,n}$) and Sullivan (Nucl. Science Eng. 70 (1979) 294) (σ_{n,n_1}) are compared with theoretical calculations (solid lines) in terms of optical model and Hauser-Feshbach-model.

Fig. 10 Excitation function for ^{28}Si(n,d_0). Calculations in terms of statistical model (H-F) and direct reaction (DWBA) are compared with experimental data.

Fig. 11 Same as in Fig. 10 for ^{28}Si(n,d_1+d_2).

Fig. 12 Angular distribution of the deuteron transition d_0 from $^{28}Si(n,d)$ at 21.3 MeV neutron incident energy. Calculated results in terms of statistical model (H-F) and direct reaction model (DWBA) are compared with experimental data.

Fig. 13 Same as in fig. 12 for deuteron groups d_1+d_2.

Fig. 14 Same as in fig. 12 for deuteron group d_3.

Fig. 15 Same as in fig. 12 for deuteron group d_4.

Fig. 16 Same as in fig. 12 for deuteron groups d_5+d_6.

Fig. 17 Excitation function for $^{28}Si(n,d)$. Calculations by present work (H-F) are compared with ENDF/B-IV.

Fig. 18 Excitation function for $^{28}Si(n,\alpha)$. Experimental data are compared with calculations by present work (H-F) and previous evaluations (ENDF/B-IV).

Fig. 19 Excitation function for $^{28}Si(n,\alpha_0)$. Experimental data are compared with calculated results obtained by statistical model (H-F) and direct reaction model (DWBA) as well as evaluated data by ENDF/B-IV.

Fig. 20 Same as in fig. 19 for $^{28}Si(n,\alpha_1)$.

Fig. 21 Same as in fig. 19 for $^{28}Si(n,\alpha_2)$.

Fig. 22 Same as in fig. 19 for $^{28}Si(n,\alpha_3)$.

Fig. 23 Same as in fig. 19 for $^{28}Si(n,\alpha_4)$.

Fig. 24 Angular distribution of the α-particle transition α_0 from $^{28}Si(n,\alpha)$ at 14 MeV neutron incident energy. Calculated results in terms of statistical model (H-F) and direct reaction model (DWBA) are compared with experimental data.

Fig. 25 Same as in fig. 24 for α_2-transition.

Fig. 26 Same as in fig. 24 for α_3-transition.

Fig. 27 Same as in fig. 24 for α_4-transition.

Fig. 28 Same as in fig. 24 for α_0-transition at 21.3 MeV neutron incident energy.

Fig. 29 α-particle emission spectrum from $^{28}Si(n,\alpha)$ at 14.8 MeV neutron incident energy. Calculated results are compared with experimental data.

Fig. 30 Excitation function for $^{29}Si(n,\alpha_0)$. Calculations in terms of statistical model (H-F) and direct reaction model (DWBA) are compared with experimental data.

Fig. 31 Same as in fig. 30 for $^{29}Si(n,\alpha_1)$.

Fig. 32 Angular distribution of α-particle transition α_0 from $^{29}Si(n,\alpha)$ at 5.85 MeV neutron incident energy. Calculated results (H-F, DWBA) are compared with experimental data.

Fig. 33 Same as in fig. 32 for α_1-transition.

Fig. 34 Excitation functions for neutron-induced production of deuterons, tritons, and α-particles in ^{28}Si. Calculations (H-F) are compared with evaluations and experimental results.

Fig. 35 Same as in fig. 34 for $^{28}Si(n,n'p)$ and $^{28}Si(n,pn)$.

Fig. 36 Same as in fig. 34 for $^{28}Si(n,n'\alpha)$ and $^{28}Si(n,\alpha n)$.